UC San Diego

UC San Diego Electronic Theses and Dissertations

Title

Investigating natural control signals for brain-computer interfaces /

Permalink

https://escholarship.org/uc/item/81t7z1cc

Author

Koerner, Adam S.

Publication Date

2013

Peer reviewed|Thesis/dissertation

eScholarship.org Powered by the California Digital Library
University of California

UNIVERSITY OF CALIFORNIA, SAN DIEGO

Investigating natural control signals for brain-computer interfaces

A dissertation submitted in partial satisfaction of the
requirements for the degree
Doctor of Philosophy

in

Neuroscience, with a Specialization in Computational Neuroscience

by

Adam S Koerner

Committee in charge:

Professor Virginia de Sa, Chair
Professor Marta Kutas
Professor Scott Makeig
Professor Jaime Pineda
Professor Terry Sejnowski

2013

Copyright
Adam S Koerner, 2013
All rights reserved.

The dissertation of Adam S Koerner is approved, and it is acceptable in quality and form for publication on microfilm and electronically:

_____

_____

_____

_____

_____

Chair

University of California, San Diego

2013

DEDICATION

To Maria for her love and support, and for being awesome.

And to my parents, for teaching me to always finish what I start.

TABLE OF CONTENTS

Signature Page iii

Dedication iv

Table of Contents v

List of Figures viii

List of Tables x

Acknowledgements xi

Vita xiii

Abstract of the Dissertation xiv

Chapter 1 Introduction 1
1.1 Background 3
1.1.1 Current issues with motor-imagery-based BCIs . . . 3
1.1.2 Error-related signals 5
1.1.3 Emotion Recognition 7
1.2 Significance 8
1.3 Dissertation Overview 9
1.3.1 Summary of Chapter 2 9
1.3.2 Summary of Chapter 3 9
1.3.3 Summary of Chapter 4 10
1.4 Contribution of Work 11

Chapter 2 A novel method to integrate error detection into sensorimotor-rhythm BCIs 12
2.1 Chapter Abstract 12
2.2 Introduction 13
2.3 Related Work 13
2.4 Methods 15
2.4.1 Subjects 15
2.4.2 Experimental Setup 16
2.4.3 Data Analysis 17
2.4.4 Error signal integration 19
2.5 Results 21
2.5.1 Classification Results 21
2.5.2 Simple combination of both classifiers 23
2.5.3 Online Simulation 24

2.6 Discussion . . . 26
2.7 Chapter Acknowledgement . . . 27

Chapter 3 The effect of real-time positive and negative feedback on motor imagery performance . . . 28
3.1 Chapter Abstract . . . 28
3.2 Introduction . . . 29
3.3 Material & Methods . . . 30
3.3.1 Subjects . . . 30
3.3.2 Experimental Setup . . . 31
3.3.3 Data Analysis . . . 32
3.4 Results . . . 34
3.4.1 Motor-imagery classification results . . . 34
3.4.2 Classification performance of subsequent test trials is correlated with feedback performance given during the training trials but not with feedback performance given during the test trials . . . 34
3.4.3 Right vs left cursor movement alone is barely classifiable . . . 37
3.4.4 The differences between positive or negative valence feedback blocks are classifiable . . . 39
3.4.5 Lateralized mu desynchronization is stronger during positive valence feedback blocks . . . 40
3.4.6 Positive valence feedback blocks are more consistent 42
3.5 Discussion . . . 44
3.6 Chapter Acknowledgement . . . 45

Chapter 4 Utilizing user satisfaction as a control signal for an online BCI . . . 46
4.1 Chapter Abstract . . . 46
4.2 Introduction . . . 46
4.3 Methods . . . 48
4.3.1 Subjects . . . 48
4.3.2 Experimental Setup . . . 48
4.3.3 Data Analysis . . . 50
4.4 Results . . . 52
4.4.1 Online Performance . . . 52
4.4.2 Offline Classification Analysis . . . 54
4.4.3 Distinguishing between methods . . . 56
4.4.4 Evaluation of satisfaction signal . . . 58
4.4.5 Evaluation of error signal . . . 60
4.5 Discussion . . . 64
4.6 Chapter Acknowledgement . . . 65

Chapter 5 Contribution of Work 66

Bibliography 69

LIST OF FIGURES

Figure 2.1: Average trace of ERPs at electrode FCz associated with cursor changes in direction 22
Figure 2.2: Classification accuracy for each subject 23
Figure 2.3: Comparison of classifier accuracy (a), trial duration (b), and ITR (c) for motor imagery alone, motor imagery with variable step size, error correction and error integration 25

Figure 3.1: Classification rate across block compared to visually presented block feedback success rate. 35
Figure 3.2: Change in correlation between classification performance and feedback success rate of training (a) and test (b) data as temporal distance increases between trained and tested data. 37
Figure 3.3: Representative common spatial patterns used for classification for classifying between right and left cursor movements. Notice that spatial patterns are centrally or dorsally located. 38
Figure 3.4: Representative common spatial patterns used for classification between right vs left motor imagery for Subject 5 trained on successful blocks. 39
Figure 3.5: Representative common spatial patterns used for classification for classifying between positive and negative blocks. Notice that spatial patterns are generally centered around the parietal and frontal lobes. 40
Figure 3.6: Grand average scalp maps for difference in theta (A) and alpha (B) band power between blocks with positive and negative feedback valence 42

Figure 4.1: Target hit rate for each method across subjects during online performance for unaided blocks. DS results include satisfaction signals as detailed in “Data Analysis". 52
Figure 4.2: Classification rate for each method across subjects during online performance for aided and unaided blocks. DS results include satisfaction signals as detailed in “Data Analysis". 53
Figure 4.3: Online ITR for each method during controlled blocks in bits/min. Note that DS results include satisfaction signals as outlined in “Data Analysis". 54
Figure 4.4: Post-hoc offline motor imagery classification accuracy with data pre-processing. Notice that aided blocks generally have better performance than unaided blocks. 55
Figure 4.5: Post-hoc offline motor imagery classification accuracy validated with 10-fold cross validation. 56

Figure 4.6: Grand average scalp maps for the statistically significant ($p<0.05$) difference in theta (A) and alpha (B) band power between good/early and bad/late blocks for the DS method. 58
Figure 4.7: Grand average scalp maps for the difference in theta (A) and alpha (B) band power between good/early and bad/late blocks for the RL method. 59
Figure 4.8: A: Grand average trace of ERPs at electrode FCz associated with cursor changes in direction for the RL method. B: Grand average trace of the ERPs at electrode FCz associated with positive and negative cursor movements (not necessarily a change in direction). . . . 62
Figure 4.9: A: Grand average trace of ERPs at electrode FCz associated with cursor changes in direction for the DS method. B: Grand average trace of the ERPs at electrode FCz associated with positive and negative cursor movements (not necessarily a change in direction). . . . 62
Figure 4.10: A: Grand average trace of FCz for correct changes in direction. B: Correct cursor movements (not necessarily a change in direction. C: Incorrect changes in direction. D: Incorrect cursor movements (not necessarily a change in direction) 63

LIST OF TABLES

Table 2.1: Feedback potential classification accuracy 23

Table 3.1: Correlation coefficient between the motor-imagery classification error rate and the pre-determined feedback failure rate within blocks. . 34

Table 3.2: Correlation coefficient of motor imagery classification performance of tested data with visual feedback success rate of trained (row 1) and tested data (row 2). Asterisks indicate significance ($p<0.05$) . . 36

Table 3.3: Classification accuracy when distinguishing between blocks with positive and negative visual feedback valence. Classification was performed using CSPs calculated on data bandpassed from 4-12Hz . . . 39

Table 3.4: Ratio of large Laplacian-filtered C3 to C4 mu power during right- and left-hand motor imagery for each subject. Mean values reflect the ratio of mean C3 across all subjects to the mean C4 across all subjects. 41

Table 3.5: Changes in classification accuracy according to trained data. When trained on the same block, results were validated using 10-fold cross-validation. Blocks with positive feedback valence are listed first. Averages are listed in bold. 43

Table 4.1: Subject-reported satisfaction with online BCI performance during controlled blocks. 53

Table 4.2: Post-hoc offline classification accuracy discriminating between DS vs RL methods. 57

Table 4.3: Post-hoc offline motor imagery classification accuracy when trained on the opposing method (DS on RL, RL on DS), blockwise cross-validated and over the whole data. 57

Table 4.4: Post-hoc offline classification accuracy for positive versus negative cursor movements. All results are statistically significant ($p<0.01$). Each letter feature corresponds with the features from “Data Analysis". 60

Table 4.5: Post-hoc offline classification accuracy for positive versus negative changes in direction. All results are statistically significant ($p<0.01$). Each letter feature corresponds with the features from “Data Analysis". 60

ACKNOWLEDGEMENTS

I would like to thank Professor de Sa for all of her support and guidance. I have learned a lot during my tenure in her lab, and it was through her that I was introduced to these areas of research. Her knowledge and insights have been instrumental in my professional progress and growth.

I would also like to thank the rest of my committee. Early on in graduate school I spent a quarter rotating with Marta Kutas, where I had the good fortune to work with her and Tom Urbach, which helped instill in me the details and experimental rigor required for EEG-based experiments. I also am thankful to have had the opportunity to work with Scott Makeig. Through him and his lab (particularly Christian Kothe) I was able to learn about a number of novel analysis techniques, as well as how to effectively communicate my research. I would also like to thank Professor Pineda for his guidance, and Professor Sejnowski for his guidance and insights into computational neuroscience.

I would also like to thank the current and former members of the de Sa lab who have provided so much support and guidance along the way. In particular, Paul Hammon, Eunho Noh, Priya Velu and Matt Valdivia have been wonderful colleagues, and have helped make much of this work possible.

Additionally, no work would get done without proper funding. My research has received funding from: NSF Grant SBE-0542013 and and SMA-1041755 to G.W. Cottrell, NSF Grant DGE-0333451 to G.W. Cottrell/V. de Sa, NSF Grant CBET-0756828 to V. de Sa and NSF Grant IIS-1219200 to V. de Sa. In addition, I have received support from the San Diego Fellowship, the NSF IGERT Fellowship, the INC Predoctoral Fellowship and the Socrates GK12 Fellowship.

The text of Chapter 2 is currently in the submission process for publication. The dissertation author is the primary author for this publication, titled “A Novel Method to Integrate Error Detection into Sensorimotor-Rhythm BCIs”, revised and resubmitted for publication in *IEEE Transactions on Neural Systems and Rehabilitation Engineering*.

The text of Chapter 3 is currently in the submission process for publication. The dissertation author is the primary author for this publication, titled “The effect of real-time positive and negative feedback on motor imagery performance”, revised and resubmitted for publication in *Frontiers in Human Neuroscience*.

In addition, Chapter 4 is currently being prepared for publication.

VITA

2007	B. S. in Bioengineering, University of Washington, Seattle
2013	Ph. D. in Neuroscience, *Specialization in Computational Neuroscience*, University of California, San Diego

PUBLICATIONS

Koerner, Adam S; de Sa, Virginia R. A Novel Method to Integrate Error Detection into Sensorimotor-Rhythm BCIs. Revised and Resubmitted. *IEEE Transactions on Neural Systems and Rehabilitation Engineering*

Koerner, Adam S; Zhang, Qiong; de Sa, Virginia R. The effect of real-time positive and negative feedback on motor imagery performance. Revised and Resubmitted. *Frontiers in Human Neuroscience*.

Koerner, Adam S; de Sa, Virginia R. Utilizing user satisfaction as a control signal for an online BCI. In Prep.

ABSTRACT OF THE DISSERTATION

Investigating natural control signals for brain-computer interfaces

by

Adam S Koerner

Doctor of Philosophy in Neuroscience, with a Specialization in Computational Neuroscience

University of California, San Diego, 2013

Professor Virginia de Sa, Chair

EEG-based brain computer interfaces (BCI) allow users to communicate with the outside world directly through signals read from the cortex. These systems typically require user training to generate signals appropriate for use. However, user ability to control such a system is variable and the variables involved are not fully understood.

In this work, we present the foundation for the identification and use of feedback-related EEG signals to both augment existing motor imagery BCIs as well as to provide a novel mechanism for control. We conducted a simulated online experiment where users were instructed to move a cursor in one dimension from the center of the screen towards a target located at the left or right extremes. In Chapter 2 we demonstrate how local aspects of visual feedback (on a single cursor movement scale) can augment existing systems or provide control signals for novel ones.

In Chapter 3, we demonstrate how global aspects of visual feedback can affect motor imagery performance. Rather than more positive feedback valence providing a more stable signal for motor imagery classification (as originally thought), feedback valence instead appears to rotate the motor imagery feature space.

In Chapter 4 we validate our findings from Chapter 2 in an online, real-time setting. In addition, we demonstrate the utility of a BCI system that utilizes local aspects of user satisfaction and dissatisfaction as a principal control signal. This proves to be a useful, stable system that provides improvement over a traditional motor imagery paradigm.

Chapter 1

Introduction

Brain-computer interfaces (BCIs) are systems that collect and interpret neural information for the purpose of controlling an object. Typically this object is either a computer program or machine, such as a robotic limb or wheelchair. A BCI system consists of several main components: brain signal acquisition, user task, signal processing and classification, user feedback, and performance of a system-controlled action. BCIs can utilize neural signals collected invasively or non-invasively. While invasive BCIs have a very good signal-to-noise ratio (SNR), their high barrier to use (surgery, unease with the idea of a neural implant), lessens their utility for the general population. This dissertation will focus on the use and utility of non-invasive BCIs, specifically those that use electroencephalography (EEG). These systems typically require user training to generate distinct and reproducible brain waves. Although EEG has low SNR, with sophisticated feature extraction techniques, we can successfully elicit useful information [1, 2, 3].

One class of BCI involves the detection and analysis of the P300 event-related potential (ERP). The P300 (or P3) wave is an endogenous potential, elicited in the process of decision making. It is usually elicited using an oddball paradigm, where low-probability target items are mixed with high-probability non-target items [4, 5]. This property can be exploited for use in a BCI. This is most often used in a typing program called the 'P3 speller' [6, 7]. In this paradigm, a grid of characters is presented, and the subject is instructed to fixate on the character they wish to type. Rows and columns flash randomly while the user counts the number of flashes for the desired character.

Once a P300 potential is detected for the chosen character, that character is output and the subject fixates on the next character. The system proceeds in this fashion until the message is finished. This system is very effective for communication, but the bit rate can be low and not everyone is able to use them effectively [8].

Another class of BCIs is the steady-state visually evoked potential (SSVEP)-based BCI. This system relies on the SSVEP, which is an EEG signal associated with retinal stimulation from 3.5 to 75 Hz [9]. Electrical oscillations in the occipital cortex are directly related to the frequency of stimulation on the retina. SSVEP-based BCIs exploit this by employing a grid of lights flashing at different frequencies. By fixating on a particular light, users can output commands to the desired system. This system is good for control, but response times can be slow [10, 11].

Another popular class of EEG-driven BCI systems is based on imagined movement. In these systems the user interacts with a computer through motor imagery, such as the imagination of hand versus foot movement. This motor imagery can then be used to output a command, such as moving a cursor on a screen to a desired destination. For the purpose of this dissertation, we will focus on this type of BCI.

Many BCI systems employ imagined movement [12, 13, 14, 15] and look for changes in mu strength, specifically decreases in frequency band power time-locked to certain events. This is called event-related desynchronization (ERD). The mu rhythm is a biorhythm which can be found in the range of 8-13 Hz over portions of motor cortex. During rest, the mu rhythm is pronounced, but during real or imagined movement, some synchrony is lost and the amplitude is diminished. This pattern, along with spatial filtering can be exploited to classify between different motor imageries. However, the success rates of these systems vary widely among the user population [16]. The factors involved in this variability are not fully understood.

Another critical issue in practical BCI use is the non-stationarity of the EEG signals [17]. EEG signals may change drastically from off-line training to on-line use as well as due to state changes in the user or drift of skin conductance. This drift can lead to loss of control of the BCI which leads to frustration and further drift of EEG signals from their training baselines [18].

Addressing these issues requires a system that acts upon more natural control

signals and is more robust towards pattern drift and user control. Here we investigate the feasibility of a more complete integration between an online BCI system controlled solely by the user's satisfaction with system performance. To this end, we investigate the integration of error-related signals and feedback responses into an online BCI system. We then compare its performance, both within and between subjects, to a traditional right vs left system.

1.1 Background

1.1.1 Current issues with motor-imagery-based BCIs

The aforementioned mu rhythm is the primary control signal for motor imagery BCIs. During rest, the mu rhythm is pronounced, but during real or imagined movement, ERD occurs. There have been a variety of different BCI systems built which employ imagined movement [12, 13, 14, 15] and look for changes in mu strength and other related features. These systems require long training times or have variable success rates with some users unable to control the system. In our own experiments with naive untrained subjects with little off-line training of the system, some subjects are not able to show classification performance above chance using the same signal processing and machine learning algorithms that give 10% error for the best subjects [15]. Also, even the subjects who are best able to control the system, have periods of loss of control.

User variability

As with any task, there has been a high level of variability in the level of control obtainable from user to user. There are many factors that contribute to BCI performance, which may vary between users, or even within the same user over multiple training sessions. This has been recorded in several different systems, and the reasons for this variability are not understood [19, 20, 21, 22]. Factors that may affect performance include mood, motivation, attention, the constraints of the environment or even brain topology [19]. Not all of these factors may be controlled for, but some can be mitigated with proper experimental design and environmental control. However, unique brain

topology and functionality can still lead to disparities in neural activity that cannot be properly controlled for with existing feature extraction techniques. Since EEG activity relies on the sum of electrical activity from populations of neurons, only a small amount of neural activity actually reaches the scalp. As a result, EEG is only sensitive to dipoles of a certain orientation. Due to differences in brain topology, folding may cause relevant dipoles to be undetected in EEG for some individuals. This leads to greater difficulty in controlling a BCI.

As it has been demonstrated that some subjects are unable to gain sufficient, usable control over motor imagery-based BCIs, there has been exploration into alternate control modalities that would allow these subjects to control a BCI using alternate means. It has been noted that in order to facilitate universal satisfactory control, it may be necessary to tailor the cognitive task towards each individual subject [23]. This may take the form of using motor imagery as the control signal for some subjects, while implementing a visual task for someone else. For example, one may use the steady state visual evoked potential (SSVEP) as a control signal as opposed to motor imagery [22].

This approach of varying a control signal for some subjects can also be advantageous for tailoring a BCI towards the strengths of disabled users. For example, it may not be the best strategy to utilize a motor imagery-based BCI for a patient who has been paralyzed for many years.

Alternately, there has been research into the effect of feedback modality on BCI control. It is well established that feedback has a profound effect on BCI performance [24, 25]. The form this feedback should take has also been studied. In one study, researchers analyzed the difference in performance between subjects utilizing visual versus auditory feedback. They found that subjects receiving visual feedback had superior performance to those receiving auditory feedback. In addition, combining both visual and auditory feedback for the same subjects results in slightly improved performance [25]. There has also been a study investigating the utility of vibrotactile feedback to either the right or left upper limb. They found that subjects were able to control a cursor significantly above chance when utilizing only haptic feedback [26]. This can be very useful for patients with visual and auditory impairments, such as those with late-stage amyotrophic lateral sclerosis (ALS).

EEG signal non-stationarity

Over time, the non-stationarity of the EEG signals [17] can also cause problems with task classification. This property can lead to loss of control of the BCI which leads to frustration and further drift of EEG signals from their training baselines [18]. These issues can be due to shifts in background brain activity, varying mental states or even due to the subject changing task strategy [27]. In order to compensate for this drift, many studies have demonstrated the value of using adaptive classifiers that update throughout the task in order to provide accurate task classification [17, 28].

However, while the features motor imagery BCIs are reliant on (ERD and event-related synchronization (ERS)) have been shown to be non-stationary, it is observed that event-related potentials (ERPs) are instead rather stationary components of an EEG signal [29]. This indicates that possible systems for mitigating this non-stationarity could make use of ERP signals as part of the proposed control signal.

These findings motivate our goal of finding other, natural control signals that can be used for EEG-based brain-computer interfaces in order to compensate for these current issues.

1.1.2 Error-related signals

There has been a substantial amount of research on investigating the neural correlates of errors during active tasks. There are a few established ERPs associated with observed errors. For the purpose of this work, we will primarily focus on the feedback-related negativity (FRN) [30, 31, 32] and the P300 [33, 34]. The FRN is a time-locked negativity 200-300 ms following an incorrect visual stimulus, centered around the anterior cingulate cortex [35]. The P300 is a positivity occurring 300-400ms following an unexpected stimulus. Both are centered in the fronto-central area of the scalp, and their amplitudes vary with respect to feedback probability. Specifically, higher probability events result in smaller perturbations [35, 36].

Error-related signals present a usable, detectable signal for single trial analysis. Integration of these into human-computer interface systems is not a new concept. For example, Parra and colleagues used these potentials during a speeded, forced decision

task where the subject physically pushes a button. Error detection was applied to remedy subject errors, and improved average system performance by 21% [37]. Zander and colleagues [38, 39] have also used detected error signals as a way to correct machine-induced errors in another task where the user physically pushes a button as their primary mode of interaction. On certain trials the computer would induce an error but the error could be corrected if a passive EEG-based BCI system correctly detected an error signal from the user's brain. Zander and colleagues were able to correct machine-induced errors with a reliability of 84%. This shows that the efficiency of an underlying system could be improved significantly with an automated error correction based on the detection of error responses.

Ferrez and Millán detected error potentials that occurred when a user controlled a cursor by manually pushing left and right keys [40]. Chavariaga and Millán showed how to modify the policy of an independent automatic agent by recognizing single-trial error potentials. They used the error recognition to modify the probability of selecting that action on the next step. The system learned over 10-50 steps in which of two directions to move [41].

Error related signals have also been investigated in motor-imagery based BCIs [42, 43] using both offline [43] and online [42] integration of error potentials in a motor-imagery based BCI. Artusi and colleagues utilize error detection in order to alter the BCI response after the entire trial is over, thus utilizing it as a post-hoc correction mechanism [42]. After each cursor movement (every 2 seconds) the EEG is tested for an error potential; if the classifier detects an error potential, the previous motor imagery cursor step is canceled. During the error potential recognition window, no motor imagery is performed. In the work by Kreilinger and colleagues, motor imagery is performed for several seconds and then the result is observed by the user and EEG is monitored for error potentials. In both of these systems the motor imagery and error recognition are performed on separate sections of the EEG. In this thesis we investigate whether we can classify error potentials recorded while a subject is trying to control a BCI with motor imagery.

1.1.3 Emotion Recognition

Another useful signal for a potential hybrid system relies on the recognition of positive and negative emotional states. Previous research has demonstrated distinct frontal lateralization in alpha power for positive and negative emotions as evoked by internal generation in frontal EEG [44, 45]. Left-lateralization tends to correspond to positive emotions and right-lateralization to negative emotions. This lateralization indicates that spatial filtering, coupled with alpha bandpower calculation can be very effective for the single-trial classification of emotions.

However, other studies have been unable to replicate these results. These studies typically utilized passive intake of external stimuli, as opposed to internally generated emotions. In one study, viewing negative and positive pictures failed to generate consistent frontal asymmetry for positive and negative emotions [46]. Similarly, emotions induced via affective auditory stimuli [47] also failed to produce these frontal spatial patterns. However, there is some indication that changes in theta during the earliest periods of emotion perception are most relevant, and these studies pointed towards the most salient features being located in the anterior regions of the brain [47, 48].

Further study has pointed to the non-linear nature of emotion-related EEG signals. Onton and Makeig have looked at the EEG-based recognition of different emotional states by analyzing modulator patterns, calculated using a combination of independent component analysis and wavelet transforms [49]. Independent component analysis (ICA) was performed on 256-channel EEG data, which was then decomposed using a wavelet transform. The resulting spectrographic data was then decomposed into 100 independent modulator patterns (IMs). These IMs were classified using k-nearest neighbors to find the closest emotion vector (from mean template data) for each of the 15 emotions. Despite considerable variability across emotions and subjects, they were able to correctly classify emotions with over 50% accuracy (chance being 7%).

Studies that examine emotional response evoked by task performance have produced more consistent results. During a task where subjects were instructed to decide between two targets that provided a reward with varying probability, response to losses (as compared to rewards) demonstrated a centralized frontal increase in theta power (4-7Hz) and phase coherence for losses [36].

In addition, during a modified version of the Wisconsin card sorting task (where subjects are instructed to match a target card to one of four “key" cards based on a given matching criterion), broad spatial increases in theta (4-6Hz) were reported after the first positive feedback, as well as increases in frontal beta-gamma (20-30Hz) frequencies [50]. This increase in theta has a different spatial distribution from the results in [36], and thus likely represents separate neural mechanisms.

Data collected simultaneously with EEG and fMRI have also demonstrated the neural structures (specifically the rostral anterior cingulate cortex, the posterior cingulate cortex, right superior frontal gyrus and striatum) that are activated more strongly for positive than for negative feedback. This was elicited during a time estimation task where subjects were instructed to estimate when one second had passed, followed by informative (positive or negative, based on performance) or uninformative feedback [51].

These studies indicate that, as would be expected, emotional responses are incredibly complex signals that can possibly be harnessed to help inform and control a BCI.

1.2 Significance

The studies cited above have demonstrated the power and limitations of motor-imagery-based BCIs. Although the utility of these BCIs are very useful, there are still drawbacks that need to be addressed. These drawbacks include user variability in BCI control and EEG signal drift. Here, we propose methods that address and mitigate these issues with motor-imagery-based BCIs.

We review the current literature on analyzing and detecting emotion and other feedback-related signals. These results indicate that these signals could be used to enhance or even provide the control signal for active BCIs.

In this work we build upon existing literature and present a method for the integration and utilization of feedback-related signals for communication and control within a brain-computer interface. This method utilizes differences in EEG signals during positive and negative emotions, as well as ERP patterns associated with viewing and processing incorrect system output.

1.3 Dissertation Overview

1.3.1 Summary of Chapter 2

In Chapter 2 we discuss a new method for integration of error-related signals into motor-imagery based BCIs. In previous systems, the detection of an error potential is used to cancel out the previous movement [42, 41] or to change the future policy [41]. In this chapter, we will refer to the method of canceling the previous movement as *error correction* We refer to our method as *error integration*; it is unique in several key ways:

1. The error signal is used to advance the cursor instead of just erasing incorrect movements.

2. Instead of using a binary classifier output for cursor movement, we use confidence measures calculated from the probabilities calculated by LDA to determine magnitude and direction of the simulated cursor movement.

3. We focus on user responses to changes in direction, as ERP and classification analysis indicates that this results in a stronger response than cursor movement in a constant direction.

We demonstrate that this method results in a significant improvement in BCI performance when compared to motor imagery alone, and demonstrates improvement in information transfer rate (ITR) when compared to previously published methods for error correction in BCIs, indicating that our method could be a powerful tool for improving current BCI systems.

1.3.2 Summary of Chapter 3

Here we investigate the effect of positive and negative feedback, uncorrelated with actual user motor imagery, on the ability to control an EEG-based BCI. We utilize the same visual stimulus as in Chapter 2, with the user believing that they are in control of an online BCI, but instead attempting to control a pre-determined stimulus. This stimulus is separated into blocks of varying success rates, which affects the user's perceived performance during motor imagery.

We find that when subjects are presented with real-time positive visual feedback, their EEG signal is more easily classifiable than when they are presented negative feedback. This effect also demonstrates a significant correlation with success gradient; the more perceived success, the more discernible the signal. In addition, we discover that providing more positive or more negative feedback to the user appears to manipulate the motor imagery feature space. This causes the two conditions (more positive or more negative feedback) to not be informative for each other. This indicates a possible approach to user training, as providing a user positive feedback in order to rescue system performance during periods where he or she is losing control is likely to hurt system performance further, contrary to previous belief.

1.3.3 Summary of Chapter 4

In Chapter 4, we investigate the feasibility of an online BCI system interactively controlled by the user's satisfaction with system performance. We compare the performance of this method of control, both within and between subjects, to a traditional right vs left motor imagery system.

For this experiment, subjects are in control of an online BCI system and alternate between one of two control methods. For the first, right vs. left system (RL), the subjects control the cursor by imagining moving their right hand to move the cursor towards a right target, and their left hand to move the cursor towards a left target. The second method, dissatisfaction vs. satisfaction (DS) system, is a little different. At the beginning of each trial, the cursor moves, with random probability, to the left or to the right. The subject imagines moving their right hand when the cursor is moving in the correct direction (in order to indicate for the cursor to keep going in the current direction), and their left hand when it is moving in the incorrect direction (in order to indicate dissatisfaction with the current direction and to indicate a change in direction).

There are 10 blocks of 20 trials each (5 blocks for each method, order of appearance is randomly chosen). As in Chapter 3, following each block, we had the subjects rate their level of control from 1 to 5, where 1 represents no control and 5 represents perfect control.

Although each method demonstrated similar control rating across subjects, there

was a statistically significant preference for the DS system in terms of online performance across all subjects. This is evident when comparing information transfer rate and offline classification accuracy. Offline results demonstrate that this result is due to the integration of feedback signals (which demonstrate a high level of usability, even during RL control) as well as a higher level of interaction with the visual feedback.

1.4 Contribution of Work

Our work as described in this dissertation makes the following contributions to the field of brain-computer interfaces:

1. We propose a novel method of integrating feedback-related potentials into an online BCI, which takes advantage of varying step sizes and differences in classifier confidence.

2. The properties of real-time EEG associated with varying visual feedback during online BCI control are explored and elicited.

3. We investigate the effect of these feedback-related signals on task performance. These effects occur even when the presented feedback has no relation to actual motor imagery performance.

4. We also note that differences in motor imagery performance due to difference in visual feedback are due to a manipulation of the motor imagery feature space, rather than motor imagery consistency as originally hypothesized.

5. We present an interactive online BCI based around interaction with visual feedback. We compare this system to a traditional motor imagery-based BCI and demonstrate that it is a viable method of control.

6. We provide evidence for the utility of feedback-related signals in an online BCI system.

Chapter 2

A novel method to integrate error detection into sensorimotor-rhythm BCIs

2.1 Chapter Abstract

Here we introduce a novel technique for the integration of feedback response into a typical motor imagery BCI system. We conducted simulated online analyses to combine the visual feedback responses (error signals) and motor imagery from data collected from this offline paradigm. Our method deviates from the traditional implementation in a few key ways. First, the error signal is used to advance the cursor movement instead of merely erasing incorrect movements. Second, instead of binary classifier outputs determining cursor steps, probabilities are used as calculated by linear discriminant analysis (LDA) to determine the magnitude of the simulated cursor movement. Lastly, we focus on user responses to changes in direction, as event-related potential (ERP) and classification analysis indicates that this results in a stronger signal than cursor movement in a constant direction. We demonstrate that this method results in a significant improvement in BCI performance when compared to motor imagery alone, and demonstrates improvement in information transfer rate (ITR) when compared to previously published methods for error correction in BCIs, indicating that our method could be a powerful

tool for improving current BCI systems.

2.2 Introduction

There have been a variety of different motor imagery BCI systems that utilize changes in mu synchronization and related features in order to generate user output [12, 13, 14]. However these systems can require long training times and success rates vary widely among the user population [16]. The factors involved in this variability are not fully understood.

In order to achieve useable accuracy [52], a standard motor-imagery paradigm requires the accumulation of evidence over several overlapping or adjacent segments of data. For example, the user could have control over the lateral movement of a cursor that begins each trial in the center of the screen. The user then attempts to move this cursor, in discrete steps, towards a fixed target at either the left or right extremes of the screen. Success in a paradigm like this requires a series of correct classifications.

In addition, real-time systems involve the user observing cursor movement as the trial is progressing (as opposed to performing the experiment and having the data analyzed after the experiment). This is important as it gives the user feedback on their interpreted brain state, and is critical for the user to improve their performance. The visual feedback may also influence the the user's thoughts and EEG signal. Notably for this paper, there is a strong 'oddball' response in response to significant, novel stimuli (such as a change in cursor direction) [53]. This response may also be paired with a strong error-related negativity around 200 ms following a system error [54]. In this paper we explore a novel use of these signals for incorporation into a standard motor imagery brain-computer interface.

2.3 Related Work

Error-related signals present a useable, detectable signal for single trial analysis. Integration of these into human-computer interface systems is not a new concept. For example, Parra and colleagues used these potentials during a speeded, forced decision

task where the subject physically pushes a button. Error detection was applied to remedy subject errors, and improved average system performance by 21% [37]. Zander and colleagues [38, 39] have also used detected error signals as a way to correct machine-induced errors in another task where the user physically pushes a button as their primary mode of interaction. On certain trials the computer would induce an error but the error could be corrected if a passive EEG-based BCI system correctly detected an error signal from the user's brain. Zander and colleagues were able to correct machine-induced errors with a reliability of 84%. This shows that the efficiency of an underlying system could be improved significantly with an automated error correction based on the detection of error responses.

Ferrez and Millán detected error potentials that occured when a user controlled a cursor by manually pushing left and right keys [40]. Chavariaga and Millán showed how to modify the policy of an independent automatic agent by recognizing single-trial error potentials. They used the error recognition to modify the probability of selecting that action on the next step. The system learned over 10-50 steps in which of two directions to move [41].

Error signals have also been applied to improve performance of BCI systems that rely on signals generated by different modalities. It has been demonstrated that it is possible to integrate the detection of error-related potentials into P3 spellers in healthy [55, 56, 57] and patient populations [58]. This integration has been shown to significantly improve BCI performance.

Error related signals have also been investigated in motor-imagery based BCIs [42, 43] using both offline [43] and online [42] integration of error potentials in a motor-imagery based BCI. Artusi and colleagues utilize error detection in order to alter the BCI response after the entire trial is over, thus utilizing it as a posthoc correction mechanism [42]. After each cursor movement (every 2 seconds) the EEG is tested for an error potential; if the classifier detects an error potential, the previous motor imagery cursor step is cancelled. During the error potential recognition window, no motor imagery is performed. In the work by Kreilinger and colleagues, motor imagery is performed for several seconds and then the result is observed by the user and EEG is monitored for error potentials. In both of these systems the motor imagery and error recognition are

performed on separate sections of the EEG. In this paper we investigate whether we can classify error potentials recorded while a subject is trying to control a BCI with motor imagery.

In addition, we discuss a new method for integration of these error feedback responses into motor-imagery based BCIs. In previous systems, the detection of an error potential is used to cancel out the previous movement [42, 41] or to change the future policy [41]. Throughout this paper, we will refer to the method of cancelling the previous movement as *error correction*. We refer to our method as *error integration*; it is unique in several key ways:

A The error signal is used to advance the cursor instead of just erasing incorrect movements.

B Instead of using a binary classifier output for cursor movement, we use confidence measures calculated from the probabilities calculated by LDA to determine magnitude and direction of the simulated cursor movement.

C We focus on user responses to changes in direction, as ERP and classification analysis indicates that this results in a stronger response than cursor movement in a constant direction (Fig. 3).

2.4 Methods

2.4.1 Subjects

Seven right-handed subjects (5 female, mean age = 24) participated in the experiment. They signed an informed consent form after the study was approved by the University Institutional Review Board. All subjects were BCI naïve and untrained, save for verbal and written instructions prior to the experiment as to how to perform kinesthetic motor imagery. Subjects were misled as to the offline nature of the experiment in order to elicit stronger feedback-related responses.

2.4.2 Experimental Setup

Data were recorded using a 64-channel BioSemi ActiveTwo system with a sampling frequency of 512 Hz, bilaterally referenced to the mastoids. In addition, EOG activity was recorded at the outer canthus and below the right eye in order to monitor eye movement. All EMG electrodes were also bilaterally referenced to the mastoids.

This experiment is designed to obtain and perform offline analysis on EEG data related to the covert production of imagined movement, in addition to collecting user response to observed changes in cursor direction (visual feedback). All subjects were led to believe they were controlling a real BCI while watching a pre-determined visual stimulus. The presented stimulus consisted of a cursor moving in discrete steps to simulate a typical BCI paradigm.

Subjects were instructed to attempt to use kinesthetic motor imagery to move the cursor either right or left, respectively, with the goal of reaching a target (located at either the left or right extremes of the screen). Subjects were allowed their choice of motor imagery for each arm, but were instructed to utilize that imagery throughout the experiment regardless of perceived efficacy. The majority of subjects utilized arm circle motor imagery. Subject 6 imagined pushing a door with either arm, while subject 5 imagined twisting their wrist and simultaneously pulling.

Each trial begins with the red cursor appearing in the screen center, with the blue target at either the right or left extreme of the screen. Subjects were instructed to begin motor imagery immediately upon appearance of cursor and target. After 1.8 seconds, the cursor begins to move (in either direction) with discrete steps every 600 ms. Each trial lasts a total of 9 seconds, including time prior to initial movement (with a total of 12 cursor movements). If the cursor reaches the target prior to the end of the trial, it remains on the screen, unmoving until nine seconds have elapsed. During each trial, there is an 80% chance that the cursor will change direction once (either correctly or incorrectly). This change in direction is to induce and detect a feedback response signal. This feedback response can be either negative (indicated by a change from correct direction to incorrect direction), or positive. In order to control for differences due to instance probability, there are an equal number of correct and incorrect changes in direction throughout the duration of the experiment.

Each experiment consists of 200 trials split into 10 blocks of 20 trials each. In order to increase subject motivation they are shown a total score, which increases with each cursor movement towards the target and decreases with each movement away. This score is compared to an ever-present 'high score'; the subjects are told that if they 'beat' the high score they will be given a monetary reward.

2.4.3 Data Analysis

Pre-processing

The collected data were high-passed filtered at 1 Hz using an FIR filter, then segmented into 10 second chunks (spanning the entire length of the trial) and visually inspected for trials with excess movement artifacts (as characterized by variance from the mean data probability distribution and increase in absolute voltage). Trials with excess movement artifacts were subsequently removed. Excess voltage changes were characterized as those above 1000 μV, and high variance trials were characterized as those that varied by more than 5 standard deviations from the mean distribution. This artifact rejection was performed using the pop_autorej function from the EEGLAB package distributed by the Swartz Center for Computational Neuroscience (SCCN) [59]. The number of trials removed per subject was 38.29 ± 17.38 (out of 200).

In addition to visual inspection, Independent Component Analysis (ICA) was used to reject data artifacts. Infomax ICA [60] was trained on the epoched and filtered datasets, and the resulting artifactual components associated with muscle movements were removed based on scalp maps and spectral patterns.

Motor imagery classification (right vs left) was performed on 600 ms chunks of data, spanning the entire length of time the cursor was in one position on the screen. Feedback response signal classification (good change vs bad change in direction) was conducted on 500 ms (or 256 individual time points) of data, epoched from the time of change in direction to 500 ms after the direction change.

Feature Extraction

Spatially dependent power decrease in mu (8-13Hz) and beta (14-25Hz) frequency bands has been observed during movement, prior to movement and during imagined or covert movement. This has been used as a feature to drive commands in motor imagery and intended movement-based BCI experiments. In order to enhance this frequency information, we use the common spatial pattern (CSP) method[61] to find a set of filters that maximize the projected variance (power) for one class while minimizing it for the other class. Applying CSPs to band-pass filtered signals greatly emphasizes the spatially-segregated power decrease differences between the different classes.

Thus feature extraction for motor imagery was conducted by band-pass filtering (with a FIR filter) the data from 7-30Hz, then using the logarithmic power of three regularized CSPs [62] for each class (total 6) [61] to provide the feature set for the classifier, linear discriminant analysis (LDA)[63]. Classifier performance was validated using 10-fold cross validation, and success rate was calculated based on the number of correct versus incorrect classifications for each trial.

Feature extraction for the feedback response signal involved the combination of three classifiers [64]. Separate LDA classifiers were trained (all validated using 10-fold cross validation) for all features. The utilized features include wavelet decomposition and both the time-domain (the channel activity) and spectral activity (as given by the average power over the particular frequency band and time period) at electrode FCz. The three features were selected based on performance with previously collected pilot data on informed subjects. They were:

1. Wavelet decomposition of the signal (bandpassed from 1-10Hz prior to performing the level 5 discrete wavelet transform (DWT) with a 4-tap Daubechies mother wavelet) with the coefficients projected onto a lower dimensional subspace using Principal Component Analysis (PCA)[65] and the top 10 components retained. PCA was performed on the wavelet coefficients in order to utilize the most salient channels and frequency bands within the data while compensating for natural variation in the most effective features between subjects.

2. FCz time domain signal bandpassed from 1-10Hz, spatially filtered using a large

Laplacian filter. The large Laplacian filter around FCz subtracts 0.25 of each of the values at electrodes CPz, FC4, FC3 and AFz from the value at FCz.

3. The average power at electrode FCz bandpassed from 1-10Hz, spatially filtered using a large Laplacian filter.

We chose to focus on the signal around electrode FCz as it has been previously determined to be one of the most informative for error-related potentials [41].

2.4.4 Error signal integration

We investigated two methods for error integration with motor imagery. In the first simple “proof of concept" method, we calculated LDA classifier probabilities for both the feedback response signal (if a change in direction occured) and motor imagery classifiers, then compared them to each other. The classifier with the higher probability determined system output, which was compared against the true label to determine accuracy. If a change in direction doesn’t occur, then the motor imagery is used as the sole control signal. To determine motor imagery classifier strength, we averaged the probabilities of the motor image classifier on each classification segment. For the feedback response (only) classification, we consider only the 500 ms following a change in cursor direction. Accuracy is determined by combining the classifier probabilities to generate a prediction.

Our second method involves a simulated online analysis. For this analysis we utilize pre-calculated classification outputs (validated with 10-fold cross-validation) for every 600ms step from the entire dataset. Every time we need to classify a cursor direction change (either positive or negative), we randomly select classifier results from our error classifier. We simulate a total of 100 experiments, in order to compensate for the stochastic nature of this result selection method.

For the classification of motor imagery alone, we use classifier predictions from 10-fold cross-validation, and use those values to simulate an online system. For motor imagery alone (referred to as RvL), we sum the classifier outputs (1 for right movements, -1 for left movements) until this sum surpasses the threshold magnitude (set at 3, as in [41]). If it never reaches threshold, the classification continues for the entire trial length

and produces no output.

We also examined the effect of variable step sizes on motor imagery performance alone. For this task, instead of using the classifier outputs, we scaled the LDA probabilities for each motor-imagery classification window from -2 to 2, with an average absolute value step size of 1 (in order to offer a fair comparison with standard constant step-size RvL). We then sum these classifier confidences over the course of the trial. The system then operates the same as RvL alone.

For the simulated online integrated system, we consider an online system that classifies the given motor imagery signals in discrete windows determined by a cursor's location on screen. If the current period's classified label differs from the previous movement direction, we move in that direction on the next step. Then, during the next window select a feedback response signal of the correct valence (correct vs incorrect) and direction (right to left or left to right) from the full set of response signals of that subject elicited by the pre-determined feedback. This feedback response signal bank consists of pre-calculated classifier probabilities generated from a 10-fold cross-validation classification. The classifier confidence from the feedback response is then added to the classification confidence for the next motor imagery window as in the "variable step size" condition described above (the "correct" vs "incorrect" cursor change must be converted to "left" vs "right" for proper integration) to produce the step size and direction at this step. As the feedback classifier is more reliable and incorporates more feature extraction methods than the motor imagery classifier, the probabilities from the feedback classifier are summed before addition to form an overall measurement of classifier strength. As with the classification of motor-imagery alone, simulation continues until the trial terminates or until the added value (cursor position) reaches a threshold.

Our online *error integration* method is compared to a more standard *error correction* method, where every simulated cursor movement results in a draw from the appropriate feedback response signal bank. In this method, user response to positive and negative movements without a change in direction are drawn separately from those that correspond to a cursor direction change. Instead of additively combining the results, the feedback response signal either overrides and removes the previous step (if the cursor movement is classified as undesirable) or does not change it (if the cursor

direction change is classified as desirable). Every step has a magnitude of 1, as has been previously used [41]. To be fair in our comparison between error correction and error integration, we allow the feedback response and motor imagery to be classified simultaneously for the error correction method instead of in alternating periods (as has previously been done). This provides a more even ITR comparison between the two methods, as error integration classifies feedback response and motor imagery during the same classification window.

In order to compare system performance, there needs to be consideration given to both accuracy and time to completion. In order to incorporate both, we utilized the information transfer rate (ITR). Assuming equal accuracy for each class (as well as balanced classes), it can be calculated using [66]:

$$I = (\log_2(C) + p\log_2(p) + (1-p)\log_2((1-p)/(C-1)))/T \tag{2.1}$$

where I is ITR, p is the classification rate of each class, C is the number of classes to be distinguished and T is the unit of time for the computation.

In order to determine significance, we fit the accumulated values to a binomial distribution (with an N equal to the total number of trials), then compared to a classifier that would perform at random level, as described in [67].

2.5 Results

2.5.1 Classification Results

Comparing user response to correct and incorrect changes (combined those from right to left and those from left to right) in direction (as displayed in Fig 2.1), there is a clear error signal during incorrect changes in direction, which sums with the associated potentials generated from a correct change in direction. The dashed line indicates a subsequent movement following the change in direction (which would be in the same direction as the previous movement). Note that the difference in neural response for correct and incorrect cursor movements is present, although it is much diminished when compared to the difference immediately following a change in direction. This difference

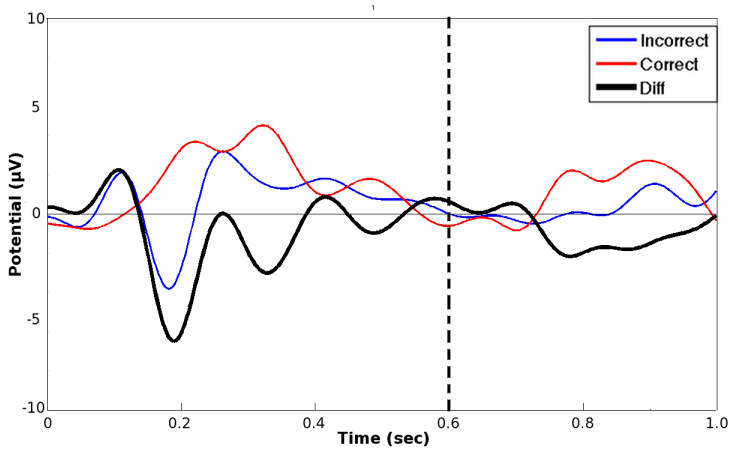


Figure 2.1: Average trace of the ERPs at electrode FCz associated with cursor changes in direction. Correct change in direction demonstrates a markedly different trace from an incorrect change, which possibly demonstrates the same complex as a correct change in direction coupled with a clear negative error potential (Ne). Vertical dashed line indicates the following cursor movement. Note that although there is a difference between the traces for subsequent good and bad movements, it is not as significant as that following the change in direction.

in neural response immediately following a change in direction also results in much greater classifiability for correct vs incorrect changes of direction when compared to classifying correct and incorrect movements that don't involve a change in direction.

We classified cursor direction change potentials associated with changes in cursor direction (desirable vs undesirable). When classifying single-trial incidence of feedback response signals, we utilized an average of the classifier outputs from the different features as described above [64]. Classification accuracy for each feature varied between subjects, with the most consistently successful being power changes from 1-10Hz over spatially-filtered FCz (4 of 7 subjects). 5 of the 7 subjects were classifiable with statistical significance for at least one feature ($p < 0.01$). Table 2.1 shows the relative classification accuracies per subject for all methods used. As illustrated in Table 2.1, by combining all features we were able to achieve statistically significant single-trial classification in 4 of 7 subjects ($p < 0.01$). Average accuracy rate for error detection across all subjects was 0.677, with the best subject having an accuracy of 0.884.

We were able to achieve statistically significant ($p < 0.01$) single-trial classification of motor imagery as described above for 4 of 7 subjects. All subjects were BCI

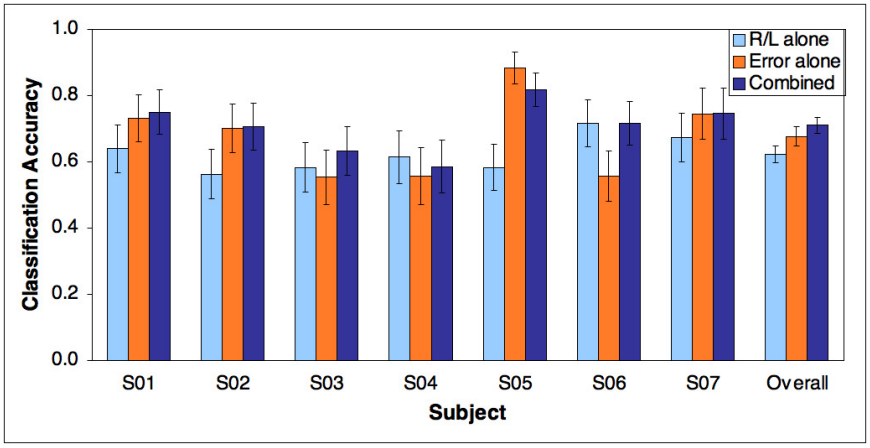


Figure 2.2: Classification accuracy for each subject, for simple right vs left classification, positive vs negative change in direction, and a simple combination of both methods. Error bars represent 95% confidence intervals.

naïve as well as task naïve. This, combined with confounding visual stimulus that could contradict actual performance, may explain low overall performance. Success rate was approximately 0.623 across all subjects, with the best subject having an accuracy of 0.716.

Table 2.1: Feedback potential classification accuracy (validated using 10-fold cross validation) for each used feature and their combined performance. (* indicates statistically greater than chance, bold font indicates most informative feature.)

	S1	**S2**	**S3**	**S4**	**S5**	**S6**	**S7**	**mean**
Wavelets	**0.694***	**0.649***	0.533	0.516	0.801*	**0.600***	0.627*	0.635*
FCz power	0.663*	**0.649***	**0.567**	0.566	**0.849***	0.593*	**0.791***	**0.666***
FCz raw	0.550	0.643*	0.493	**0.598***	0.699*	**0.600***	0.682*	0.606*
Combination	0.731*	0.701*	0.553	0.557	0.884*	0.557	0.745*	0.677*

2.5.2 Simple combination of both classifiers

In order to combine the classifiers, we compared the LDA classifier probability from both the feedback response and motor imagery systems to determine the dominant class. Motor imagery probabilities were averaged for the duration of the trial (15 classifications), which was compared to the feedback response classifier probability at the change in cursor direction. As a result, classification was significantly improved (p

< 0.01) over the motor imagery system alone as can be seen in Fig 3.1. The average accuracy for all subjects was 0.710, which is slightly above the 0.7 required for a subject to be able to feel in control of a BCI [68]. We believe that, with training, these subjects would be able to use such an integrated BCI system successfully.

2.5.3 Online Simulation

In addition to the previous, simplistic method of error integration, we also investigated the possibility of how such an integration would work in an online setting (as discussed in 3.3). Online paradigms were simulated with an N of 100 for each subject. Motor imagery classification alone using this pseudo-online paradigm results in slightly improved accuracy compared with simple classification outlined in Fig 3.1. This is due to the fact that for this method correct classification is the sum of several classifications. This may result in an early classification without relying on user performance later in the trial, when fatigue may degrade the signal. When variable step sizes are introduced (that vary directly with classifier confidence, as in our error integration method), there is a negligible change in system accuracy. However, when error integration is included, classification accuracy improves to an average of 0.790 for all subjects, as can be seen in Fig 2.3a. Error correction has a similar mean accuracy rate. As a result, 6 of 7 subjects exhibited significant improvement in classifier performance for both methods, and 5 of 7 surpassed the 0.7 generally associated with what some have called "BCI literacy", which is basically a measurement of the user's ability to control a BCI [68].

In addition, the average time to classification (with a maximum of 9 seconds before trial timeout) improved from 4.15 to 3.89 seconds with error integration (compared to 4.51 seconds with error correction). This, combined with the increase in classification accuracy, indicates a greatly improved ITR for the error integration system over motor imagery alone. The mean ITR improves from 3.88 bits/min to 5.84 bits/min with error integration (and 5.49 bits/min with error correction). Despite the differences in time to completion and with the differing methods, error integration and error correction have equivalent mean step sizes. This holds true when comparing the step sizes for simple motor imagery and when using variable step sizes, although the variable step sizes do exhibit a higher variance in user performance.

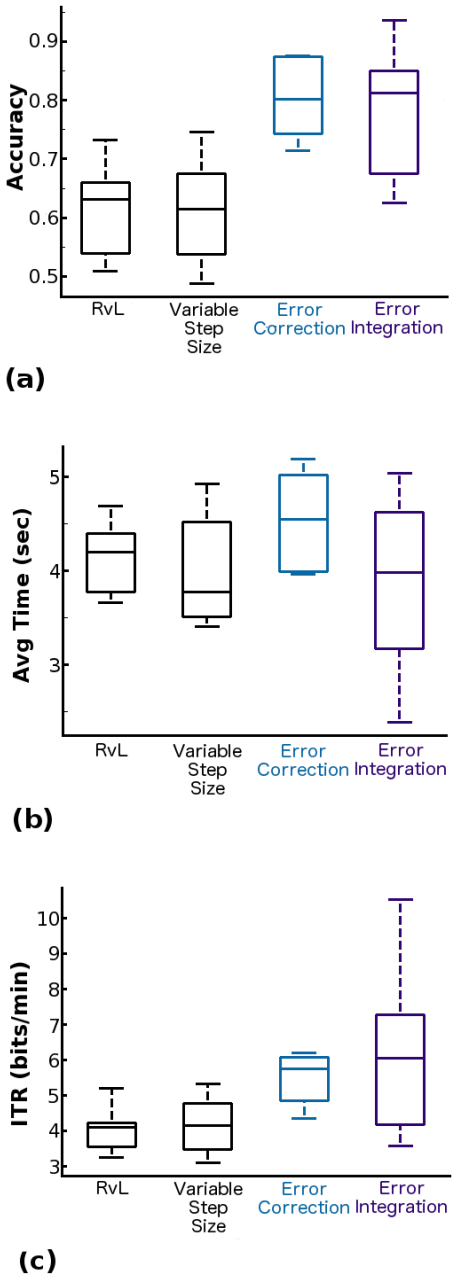


Figure 2.3: Comparison of classifier accuracy (a), trial duration (b), and ITR (c) for motor imagery alone, motor imagery with variable step size, error correction and error integration. Each box represents data for all subjects, with the central line representing the median, the box edges the 25th and 75th percentiles, and the whiskers extending to the extremes.

When comparing error integration with error correction, error integration demonstrates smaller increases in accuracy for 5 of 7 subjects (although median accuracy for error integration shows a slight improvement). However, the time required is decreased with error integration when compared with error correction. As can be seen in Fig 2.3, there is a larger amount of variance in overall ITR, accuracy and time to completion for our error integration method over the error correction method even though the average value is largely equivalent. This indicates that error integration may be the ideal solution for certain subjects but not others. While these results seem to indicate that a portion of this variation in performance between subjects is due to utilizing variable step sizes, the improvement in performance over simple error correction appears to be the result of error integration, rather than being a product of varying step sizes with classifier confidence.

2.6 Discussion

These results are promising, as they demonstrate that combining active and passive control signals for a brain-computer interface could result in improved usability for the population at large. The classification accuracy for 6 of the 7 subjects was statistically significant ($p < 0.01$) for one or both classifiers, and the combination of both classifiers resulted in statistical significance for all subjects. It is important to note that we used untrained volunteer students as subjects. This likely has an adverse effect on overall system performance, but also gives information on how this system might work with the general population. In particular, we hypothesize that with subjects trained to perform detectable motor imagery, using variable step sizes would generate a larger improvement in system performance than reported here. The presentation of sham visual stimulus probably also hurt classification performance for all methods. Adaptivity is important for these systems in order to be effective, and it hurts effectiveness if the subjects lack meaningful feedback to cue adaptation. We believe that providing subjects the ability to learn through real visual feedback in an online system would improve performance for an online version of this BCI system.

We have demonstrated that it is possible to simultaneously detect error signals

and motor imagery. This indicates that it is possible to streamline the integration of error detection by analyzing user response and motor imagery within the same classification window, rather than separating the signals as has been previously done. This could result in more efficient, effective BCI systems.

Using both feedback response and motor imagery signals is more robust from a usability standpoint and would possibly be able to allow more individuals to successfully control motor imagery-based BCI systems. In addition, implementing classifier probabilities via error integration into a motor imagery BCI seems to provide greater potential for system use as opposed to simple error correction. Some subjects performed much better with our error integration system, and it seems to have a higher ceiling in terms of ITR. This demonstrates that, for some subjects, this may be a superior system for training subjects to use a BCI, and it may improve upon the number of people who can successfully use BCIs.

A motor imagery BCI that has a greater reliance on user response to visual feedback would have a number of interesting possibilities. With both classifiers running at the same time, there are a number of modes of interactions. For example, if both classifiers agree on cursor direction, the cursor could take an even larger jump in that direction (indicating higher probability). Combined with other adjustments, such as constraining the number of direction changes occuring within a given time period (allowing subjects time to adjust to the visual feedback) could boost integrated system performance. We are currently working on integrating this error detection into a real-time BCI system that would learn along with the subject to provide improved BCI competency.

2.7 Chapter Acknowledgement

The text of Chapter 2 is currently in the submission process for publication. The dissertation author is the primary author for this publication, titled “A Novel Method to Integrate Error Detection into Sensorimotor-Rhythm BCIs”, revised and resubmitted for publication in *IEEE Transactions on Neural Systems and Rehabilitation Engineering*.

Chapter 3

The effect of real-time positive and negative feedback on motor imagery performance

3.1 Chapter Abstract

Brain-computer interfaces (BCI) are tools that interpret neural signals and translate them into actionable commands. These systems provide real-time control, and thus real-time performance feedback to the user. There has been a good deal of research into the effect of different feedback modalities on BCI control, but not into how the specific information of this feedback (i.e. subject performance) affects system performance. Here we investigate the effect of different rates of positive and negative feedback, uncorrelated with actual user motor imagery, on the ability to control an EEG-based BCI. We find that when subjects are presented with more positive real-time visual feedback, their EEG signal is more easily classifiable than when they are presented more negative feedback. This effect also demonstrates a significant correlation with success gradient; the more perceived success, the more discernible the signal. Further analysis reveals that motor-imagery from blocks with more positive valence feedback are well classified by classifiers trained on motor-imagery from other blocks with more positive valence feedback but are not well classified by classifiers trained on motor-imagery from those with

more negative valence. Interestingly, trials from blocks with more negative valence are not well classified by classifiers trained on trials from either type of blocks, but perform significantly better when trained on other blocks with more negative valence than when trained on blocks with more positive valence. We also show that EEG power in 4-12 Hz can be used to successfully classify the feedback block valence of a given trial giving further evidence that the feedback success rate has a large effect on EEG signals used for motor-imagery classification. Our results are consistent with previous results on loss of control, and provide the potential for the use of this signal in improving online BCIs.

3.2 Introduction

As BCI systems require a period of training to reach peak efficacy, there has been a lot of study into effective methods to present informational feedback to subjects controlling the BCI. For example, combining different modalities such as proprioceptive and visual feedback [69, 70] or visual and auditory feedback [25] has been shown to improve BCI performance. In addition, it is well established that the addition of feedback significantly affects the user's signal, which can cause complications when training a subject to use a BCI [27]. This indicates that training a subject utilizing similar feedback to the task may be ideal.

One study has demonstrated that presenting subjects with negative feedback following periods of motor imagery (uncorrelated with their actual performance) can actually improve the asymmetry of mu-rhythm between hemispheres during motor imagery (a common marker of successful motor imagery performance). However, this did not result in statistically significant differences in single-trial classification [71].

However, previous studies have demonstrated that online negative feedback can generate the feeling of loss of control, which has been associated with global desynchronization [20]. The effect of frustration was also studied by using an "affective Pacman" game (controlled by key presses), where user experience was perturbed during play to induce frustration. The effect was found to be particularly prevalent in the delta, theta and alpha bands over the motor cortex [72]. This desynchronization may be associated with increased workload brought on by frustration with the loss of control, which has

been characterized by spatially localized differences in alpha and theta power during n-back memory tasks [73, 74]. This loss of control in turn induces data non-stationarity, which has a profound impact on the relevant feature space for an ERD-based classifier [75, 76]. This indicates a necessity for adaptive classification in addition to possible context awareness to incorporate user state into motor imagery classification.

Previous work has investigated the effect of biased feedback on motor imagery-based BCI performance and found that negatively biased feedback impedes BCI performance [77]. However, as the feedback was still reliant on some aspect of the user's motor imagery signal, there is an inherent reflection of the user's natural ability.

Here we investigate the effect of real-time positive and negative feedback that is not the result of user motor imagery performance. Since the feedback is not causally related to the motor imagery performance, we can truly isolate the effect of the feedback from the user's motor imagery performance. This ensures that any observed feedback-related effect is not due to the motor imagery influencing the feedback but instead due to the feedback affecting the motor imagery, allowing for more complete conclusions.

We hypothesize that negative feedback will induce a feeling of losing control, which will have a negative impact on the subjects' ability to perform consistent motor imagery with a clear, discriminable motor imagery signal [75, 76]. In addition, presenting positive feedback will provide a stronger motor imagery signal, resulting in a more consistent training set for developing a motor imagery classifier. Real-time feedback is provided throughout the trial (while the subject is performing the task), and thus provides the subject constant, updated feedback during the task.

3.3 Material & Methods

3.3.1 Subjects

Seven right-handed subjects (5 female, mean age $= 22.1 \pm 2.7$ years) participated in the experiment. They signed an informed consent form after the study was approved by the University Institutional Review Board. All subjects were BCI naïve and untrained, save for verbal and written instructions prior to the experiment as to how to perform kinesthetic motor imagery. Kinesthetic (as opposed to visual) imagery has

been shown to provide a stronger ERD signal [78]. Subjects were misled as to the offline nature of the experiment in order to provide greater control over their feedback-related responses. At the end of each block, the subject was instructed to rate the level of control they felt they had over the system from a scale of one to five, where one is no control and five is perfect control.

3.3.2 Experimental Setup

Data were recorded using a 64-channel (located according to the international 10-20 system) BioSemi ActiveTwo system with a sampling frequency of 512 Hz, bilaterally referenced to the mastoids. In addition, EOG activity was recorded at the outer canthus and below the right eye in order to monitor eye movement. All EOG electrodes were also bilaterally referenced to the mastoids. No electrodes were removed during pre-processing.

This experiment is designed to obtain and perform offline analysis on EEG data related to the covert production of imagined movement, in addition to collecting user response to observed changes in cursor direction (visual feedback). All subjects were led to believe they were controlling a real BCI while watching a predetermined visual stimulus. The presented stimulus consisted of a cursor moving in discrete steps to simulate a typical BCI paradigm.

Subjects were instructed to attempt to use kinesthetic motor imagery to move the cursor either right or left, respectively, with the goal of reaching a target (located at either the left or right extremes of the screen). Subjects were allowed their choice of motor imagery for each arm, but were instructed to utilize that imagery throughout the experiment regardless of perceived efficacy. This was verbally confirmed following the experiment. The majority of subjects utilized arm circle motor imagery. Subject 6 imagined pushing a door with either arm, while subject 5 imagined twisting their wrist and simultaneously pulling.

Each trial begins with the red cursor appearing in the screen center, with the blue target at either the right or left extreme of the screen. Subjects were instructed to begin motor imagery immediately upon appearance of cursor and target. After 1.8 seconds, the cursor begins to move (in either direction) with discrete steps every 600 ms. Each

trial lasts a total of 9 seconds, including time prior to initial movement (with a total of up to 12 cursor movements - some trials will have the cursor reach a target early).

Each experiment consists of 200 trials split into 10 blocks of 20 trials each. Each block had a set '**feedback success rate**' that determined how many trials ended on the same/opposite side as the target. This value changed randomly from block to block. S1 and S2 (mean of 0.58, range from [0.25 to 0.85] received slightly different stimuli from S3-S7 (mean of 0.61 and a range of [0.35 0.9]). These rates were also randomly selected. In addition, to increase subject motivation, they are shown a total score, which increases with each cursor movement towards the target and decreases with each movement away. This score is compared to an ever-present 'high score'; the subjects are told that if they 'beat' the high score they will be given a monetary reward.

This experiment utilized sham feedback in order to elicit periods of more or less positive feelings of control. Previous work has demonstrated differences in neural response to real-time and sham feedback [79]. However, in this instance subjects were instructed prior to the session that they were receiving sham feedback, where in this case subjects were led to believe that they were receiving real-time feedback.

3.3.3 Data Analysis

Preprocessing

For post-hoc offline analysis, the collected data were high-passed filtered at 1 Hz using an FIR filter, then segmented into 10 second chunks (spanning the one second inter-stimulus interval and the entire length of the trial) and visually inspected for trials with excess movement artifacts (as characterized by variance from the mean data probability distribution and increase in absolute voltage). Trials with excess movement artifacts were subsequently removed. Extreme voltage changes were characterized as those above 1000 μV, and high variance trials were characterized as those that varied by more than 5 standard deviations from the mean distribution. This artifact rejection was performed using the pop_autorej function in the EEGLAB package distributed by the Swartz Center for Computational Neuroscience (SCCN) [59]. The number of trials removed per subject was 38.29 ± 17.38 (out of 200).

In addition to visual inspection, Independent Component Analysis (ICA) was used to reject data artifacts. Infomax ICA [60] was trained on the epoched and filtered datasets, and the resulting artifactual components associated with muscle movements were removed based on scalp maps and spectral patterns. Following cleaning, data were visually inspected for the proper removal of artifacts.

Motor imagery classification (right vs left) was performed on 600 ms windows of data. This window length was chosen as it matches the duration the cursor was in one position on the screen. Windows did not overlap.

Feature Extraction

Spatially dependent power decrease in mu (8-13Hz) and beta (14-25Hz) frequency bands has been observed during movement, prior to movement and during imagined or covert movement [61]. This has been used as a feature to drive commands in motor imagery and intended movement-based BCI experiments. In order to enhance this frequency information, we use the common spatial pattern (CSP) method[61, 80] to find a set of patterns that maximize the projected variance (power) for one class while minimizing it for the other class. Applying CSPs to band-pass filtered signals greatly emphasizes the spatially-segregated power decrease differences between the different classes [81].

Feature extraction was conducted by band-pass filtering (with a FIR filter) the data from 7-30Hz [61], then using three regularized CSPs [62] for each class (total 6) [61] to provide the feature set for the classifier, linear discriminant analysis (LDA)[63]. Classifier performance was validated using 10-fold cross validation, and success rate was calculated based on the number of correct versus incorrect classifications for each trial.

In order to determine classifier significance, we fit the accumulated values to a binomial distribution (with an N equal to the total number of trials), then compared to a classifier that would perform at random level, as described in [67, 82]. All correlations are calculated using the Pearson product-moment correlation coefficient, and their significance is determined by a t-test.

3.4 Results

3.4.1 Motor-imagery classification results

In order to test the hypothesis that feedback valence affects motor imagery discriminability, we generated (and validated by 10-fold cross-validation) individual classifiers for each block of 20 trials, instead of carrying out classification on all trials available at once. Classification accuracy within blocks are then compared with the unique underlying pre-determined feedback success rate of that block. We found a considerable level of correlation between the computed cross-validation classification accuracy of the subjects' motor imagery and the pre-determined (unrelated) block feedback success rate as shown in Table 3.1. Correlation coefficients for 4 of 7 subjects demonstrate a significant level of correlation between block success and classification rate (indicated by an asterisk in Table 3.1).

Table 3.1: Correlation coefficient between the motor-imagery classification error rate and the pre-determined feedback failure rate within blocks.

	S1	S2	S3	S4	S5	S6	S7
Correlation	0.1613	-0.2231	0.2036*	0.1606	0.4562*	0.3714*	0.3898*

The motor-imagery classification accuracy across subjects for each block is displayed in Figure 3.1, juxtaposed with the feedback block success rate. Each block's feedback success rate was determined randomly, with a mean value of 0.6. As the correlation in Table 3.1 indicates, changes in classification accuracy for most subjects appears to mirror the appropriate block success rate.

3.4.2 Classification performance of subsequent test trials is correlated with feedback performance given during the training trials but not with feedback performance given during the test trials

In order to further examine the short-term effect of feedback on motor imagery performance (and to further elicit the mechanisms for the effect of feedback valence on

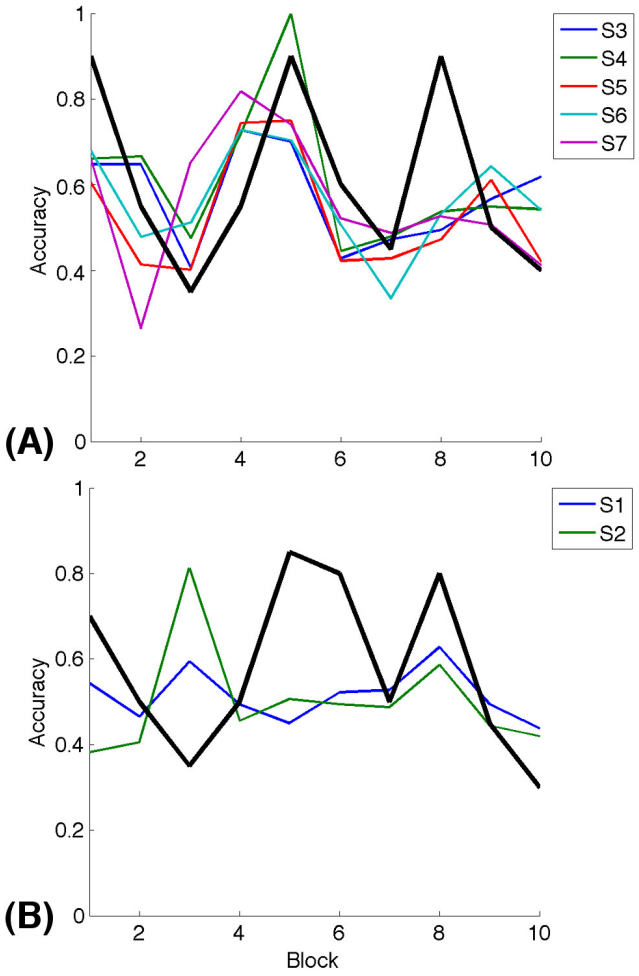


Figure 3.1: Classification rate across block compared to visually presented block feedback success rate.

classification accuracy), we performed a simulated online classification. For this analysis, we test each trial using a motor imagery classifier (as used for all other analyses) that has been trained on the previous 20 trials. For each trial, we take the first 9 time windows and test the trained classifier on those 9 steps. We choose the first nine because subsequent steps may not include motor imagery (as in some cases the subject would stop the task once the cursor hits its target, which occurs at the earliest after seven steps). We then compare the motor-imagery classification accuracy to the visual feedback performance for the trained trials and the tested trials (found in Table 3.2).

Table 3.2: Correlation coefficient of motor imagery classification performance of tested data with visual feedback success rate of trained (row 1) and tested data (row 2). Asterisks indicate significance ($p<0.05$)

	S1	S2	S3	S4	S5	S6	S7
Trained Data	0.2347*	-0.1561	0.0817	0.3050*	0.2022*	0.3949*	0.5459*
Tested Data	0.1005	-0.0638	-0.1187	-0.1317	0.1381	-0.0491	-0.0706

When analyzing the results, we found that there was a strong, positive correlation between classification performance and the feedback success rate of the trained data. This was consistent for 5 of 7 subjects. This indicates that training data is more consistent for positive visual feedback than for negative feedback. However, there was not a comparable positive correlation with visual feedback valence of the tested data. This latter result indicates that the relationship between feedback valence and motor imagery performance is more likely due to consistent training data during positive valence training.

In addition, when "drift" (additional, un-included trials between the training and test trials) is added to this protocol, the correlation between visual feedback valence in both the training data and the tested data with classification accuracy does not show statistically significant change (as shown in Fig 3.2).

Taken together, these results provide evidence for our hypothesis that the quality of the training data is specifically tied to perceived performance. This indicates that positive feedback could provide a more stable control signal for training (as hypothesized), and may be an effective way to initially train subjects. The training data obtained during regions with more negative feedback valence is not as reliable as time periods with

positive feedback valence, which may indicate that subjects are trying to change their control strategy, are getting frustrated by the experiment, or some combination of the two.

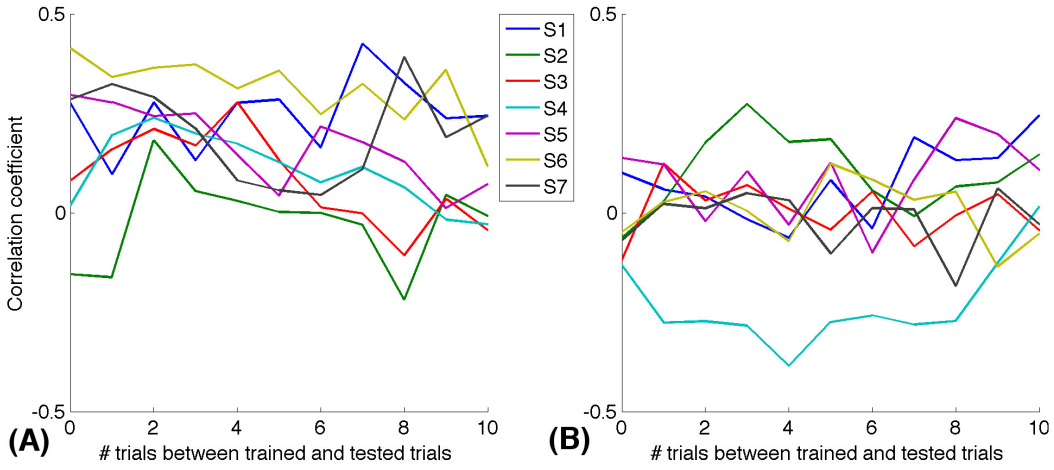


Figure 3.2: Change in correlation between classification performance and feedback success rate of training (a) and test (b) data as temporal distance increases between trained and tested data.

3.4.3 Right vs left cursor movement alone is barely classifiable

One possible explanation for this correlation in classification performance with visual feedback success could be that we are actually classifying eye movement or attentional shifts towards the desired target. During successful periods of visual feedback, if the subject is tracking the cursor movement, it is possible that any increase in task success could be due to the detection of more “correct" eye movements.

To test whether eye movements are complicit in the effect of feedback success rate on motor imagery performance, we attempted to classify right vs left cursor movement using the same classifier as for motor imagery (CSP power bandpassed from 7-30Hz). We used 750ms windows (spanning 150ms before to 600ms after each cursor movement), and the classifier was validated using 10-fold cross validation. We used this technique to attempt to classify between the two classes "right cursor movement" and "left cursor movement" in order to determine if any eye movement artifacts remain

within the data to possibly explain the improvement in classification performance for periods of positive visual feedback.

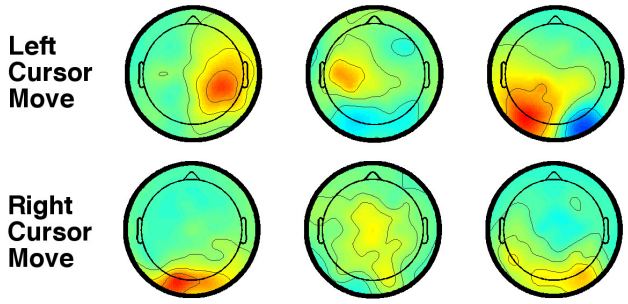


Figure 3.3: Representative common spatial patterns used for classification for classifying between right and left cursor movements. Notice that spatial patterns are centrally or dorsally located.

We find that the eye movement contribution is likely small, as attempting to classify right vs left cursor movement (regardless of target location) was difficult. Although the results were significant (mean accuracy of 0.5402 across all subjects), this is not enough to explain the difference in classification accuracy between successful and unsuccessful blocks. In addition, CSP results (as visualized in Figure 3.3) demonstrate that the most informative spatial filters for this comparison focus on the areas for visual processing and attention, not in the eye movement region.

In addition, analysis of the CSPs generated during classification of motor imagery reflect a pattern that appears to be primarily classifying on neural activity, not motor artifacts. A representative set of spatial patterns can be seen in Figure 3.4.

Another test was performed in order to determine whether the discriminative space for distinguishing right and left cursor movements would be useful for motor imagery classification. To do this we trained CSPs for cursor movements, then trained a right-vs-left motor imagery classifier using the features provided by those CSPs. This provides a way to determine whether the cursor movement CSP feature space is informative for the motor imagery feature space, thus indicating how much of the motor imagery classification results are the result of cursor movement. Following analysis of these results, it seems as though the CSPs generated for cursor movement classification are in a different feature space from motor imagery. When these CSPs generated from cursor movement classification are used to attempt to classify left vs right motor

imagery, the classifier performs at chance (mean accuracy of 0.505 across all subjects). This analysis was validated using leave-one-block-out cross-validation. This indicates that following cursor movement is likely not a factor in the differences in motor imagery classification between blocks with more positive valence and those with more negative valence.

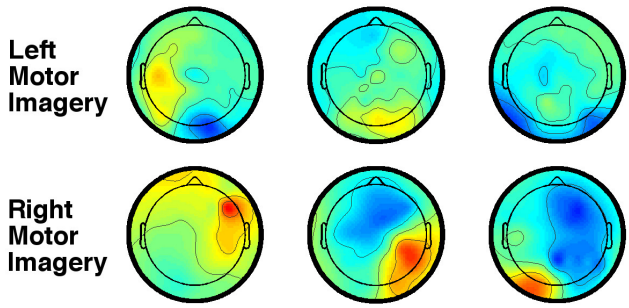


Figure 3.4: Representative common spatial patterns used for classification between right vs left motor imagery for Subject 5 trained on successful blocks.

3.4.4 The differences between positive or negative valence feedback blocks are classifiable

Table 3.3: Classification accuracy when distinguishing between blocks with positive and negative visual feedback valence. Classification was performed using CSPs calculated on data bandpassed from 4-12Hz

	S1	S2	S3	S4	S5	S6	S7	mean
Classification	0.679	0.662	0.652	0.662	0.583	0.579	0.634	0.636

In order to attempt to further investigate the differences between positive and negative blocks, we attempted to classify data according to the feedback valence of its block (positive or negative) (as seen in Table 3.3.

Another way to test our hypothesis and check for consistency of training data is to compare the results of testing motor imagery classification from a block of trials with a classifier trained on imagery from other blocks of similar valence or blocks of the other valence. For the purposes of this we defined the 5 blocks with best feedback performance to be the “positive valence” blocks and the 5 blocks with lowest feedback performance to the the “negative valence” blocks.

We performed this classification on all trials, right and left, and assigned the data to classes based on whether the trial occurred in a positive or negative block. Our feature extraction method was identical to previous experiments, except here data were bandpassed from 4-12 Hz prior to applying CSPs. These frequencies have been previously implicated in studies looking at positive and negative affective emotions [47, 48], as well as increased workload and loss of control [72, 73, 75, 83].

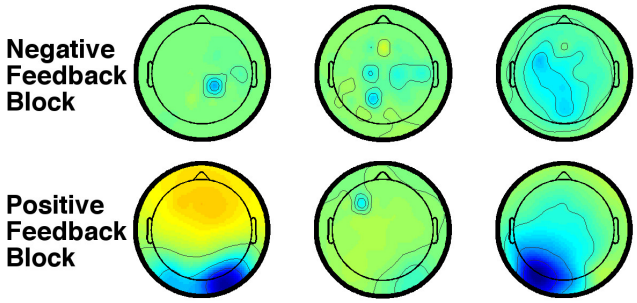


Figure 3.5: Representative common spatial patterns used for classification for classifying between positive and negative blocks. Notice that spatial patterns are generally centered around the parietal and frontal lobes.

We were able to classify between positive and negative blocks with statistical significance for each subject ($p < 0.01$). This demonstrates that there is a spatially weighted difference in EEG power in the 4-12 Hz frequency band between blocks with overall more positive or negative feedback presentation. The CSP patterns demonstrate that the most important electrodes for classification are located primarily in the parietal and frontal regions, consistent with current literature about positive and negative affective emotions. This demonstrates that our classifier is picking up on underlying base differences in neural activity that could possibly reflect changes in affected emotions or a potential increase in workload.

3.4.5 Lateralized mu desynchronization is stronger during positive valence feedback blocks

Given the correlation between system performance and block success rate, it would be expected that lateralized differences in mu desynchronization (an accepted standard for motor imagery performance) would be more pronounced during conditions

Table 3.4: Ratio of large Laplacian-filtered C3 to C4 mu power during right- and left-hand motor imagery for each subject. Mean values reflect the ratio of mean C3 across all subjects to the mean C4 across all subjects.

	S1	S2	S3	S4	S5	S6	S7	mean
Left, Pos. Feedback	1.354	1.253	1.290	1.394	1.181	1.342	1.516	1.326
Left, Neg. Feedback	1.340	1.274	1.163	1.377	1.151	1.314	1.272	1.269
Right, Pos. Feedback	1.301	1.265	1.230	1.375	1.155	1.296	1.459	1.285
Right, Neg. Feedback	1.313	1.276	1.226	1.400	1.166	1.330	1.351	1.289
Pos. R - L	**-0.053**	**0.012**	**-0.060**	**-0.019**	**-0.026**	**-0.046**	**-0.057**	**-0.041**
Neg. R - L	**-0.027**	**0.002**	**0.063**	**0.023**	**0.015**	**0.016**	**0.079**	**0.020**

with more positive feedback as opposed to those with more negative feedback. To calculate this, we utilized the measure S [71], which calculates the ratio of mu-band power of C3 to C4 for right- and left-hand motor imagery. C3 and C4 are approximately located over the 'hand' region of the left- and right-hemisphere motor cortex, respectively. Motor control is organized in a contralateral manner, meaning that control of the right side of the body is mostly controlled by the left hemisphere motor cortex, while the left side of the body is mostly controlled by the right hemisphere motor cortex. During motor imagery, there is a Therefore, we would expect a larger S to be associated with successful execution of left-hand motor imagery, and a smaller S to be associated with successful execution of right-hand motor imagery.

As can be seen in Table 3.4, with the exception of S2, subjects show the expected difference in S value between left-hand motor imagery and right-hand motor imagery during periods of more positive feedback, while only S1 demonstrates the same result during periods of more negative feedback (but even to a lesser extent than during periods of positive feedback). This different is not statistically significant, but is consistent with the observed decrease in motor imagery performance during periods of more negative feedback.

In order to account for the difference in classification between successful and unsuccessful blocks, we also looked at the difference in spectral activity between the two types of blocks. To do this, we looked at the average EEG power during motor imagery for blocks with more successful and more unsuccessful visual feedback. When we compared alpha (8-12Hz) and theta (4-7Hz) power correlated around each cursor movement (as shown in Figure 3.6), we found significant differences using a paired t-test ($p < 0.05$)

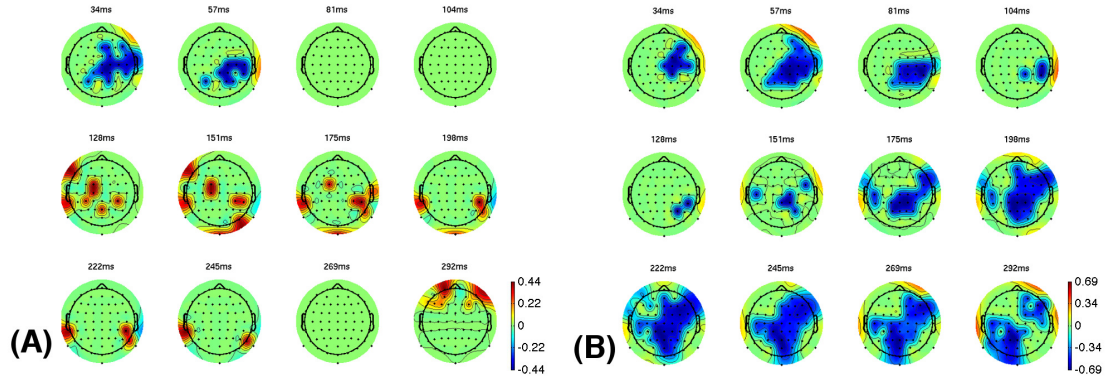


Figure 3.6: Grand average scalp maps for the statistically significant ($p<0.05$) difference in theta (A) and alpha (B) band power between blocks with positive and negative feedback valence. These figures demonstrate a strong difference in both theta and alpha power over the centro-parietal region following each cursor movement.

between user response to cursor movements. Although these results are not corrected for multiple comparisons (given the multiple channels and time points), the pattern consistency over time (particularly for the alpha band results in Figure 3.6B) indicates that they would likely remain significant when provided for multiple comparisons. In addition, given that the different data points are likely correlated, the Bonferroni method may prove to be overly conservative, and cluster analysis would be the better option. These results are presented for illustration, and not as a significant marker of neural activity.

For the alpha band, negative feedback blocks appear to have stronger spectral activity primarily in the centro-parietal regions, which have been previously implicated in studies on positive and negative emotions [44, 45] as well as increased workload induced by loss of control [83, 73]. This is in conjunction with higher parietal power in both alpha and theta frequency bands during periods of negative feedback [84]. As can be seen in Figure 3.6A, early theta band responses demonstrate significantly stronger centro-parietal spectral activity for more negative feedback blocks, but then demonstrate localized regions of higher central power for more *positive* feedback blocks.

3.4.6 Positive valence feedback blocks are more consistent

As seen in Table 3.5, motor imagery classification from positive feedback blocks trained with data from other positive feedback blocks gives better performance than

Table 3.5: Changes in classification accuracy according to trained data. When trained on the same block, results were validated using 10-fold cross-validation. Blocks with positive feedback valence are listed first. Averages are listed in bold.

Positive Blocks	1	4	5	6	8	**Pos Mean**
Same Block	0.688	0.695	0.713	0.615	0.661	**0.674**
Same Valence	0.650	0.595	0.605	0.580	0.575	**0.600**
Opposite Valence	0.580	0.538	0.535	0.533	0.530	**0.543**
Negative Blocks	2	3	7	9	10	**Neg Mean**
Same Block	0.645	0.655	0.627	0.622	0.597	**0.630**
Same Valence	0.590	0.577	0.571	0.571	0.577	**0.577**
Opposite Valence	0.533	0.532	0.528	0.541	0.535	**0.534**
						Total Mean
						0.651
						0.588
						0.538

motor-imagery classification from negative feedback blocks trained with data from other negative feedback blocks. These within-valence block hold-out results are significantly different between the more positive and more negative valence groups ($p < 0.01$).

However, when a motor imagery classifier was trained on blocks with more negative feedback valence and tested on those with more positive feedback valence (and vice versa), the classification accuracy is at random chance level, and there is no significant difference between the performance of negative valence blocks trained on positive valence blocks and vice versa.

This contradicts our hypothesis, as data trained on the more positive feedback valence does *not* create a strong motor imagery classifier for data collected during periods of more negative feedback valence. Instead, it seems that the more similar the conditions of the training data are to those during the test data, the better the classifier performance. This suggests that differences in feedback valence causes a manipulation of the motor imagery feature space, which is a novel finding that has implications for the use of this satisfaction signal in future BCI applications.

3.5 Discussion

Building on previous work, we have found that perceived subject performance has an effect on actual task performance. This appears to occur regardless of whether that feedback is grounded in actual performance. In our experiments this occurs when feedback is provided in real-time while the subject is performing the motor imagery. This can provide a good basis for training a subject new to real-time BCIs, as it may be advantageous to present the subject with initial positive feedback in order to induce a positive mental state and generate a better, more detectable control signal.

However, we also demonstrate that the signals during periods of positive and negative visual feedback have demonstrably different feature spaces. This is evidenced by the statistically significant level of classification (as seen in Table 3.3), and that classifiers trained on regions of positive or negative feedback do not classify well on data from the opposing valence. This is consistent with previous results investigating the introduction of non-stationarity induced by a loss of control [75, 76].

One explanation for the differences in user performance may be the tendency for users to change their motor imagery strategy when confronted with an ineffective system. Although users were instructed to choose one strategy and stick with it, it is possible that the negative feedback discouraged them enough to try something new. This would also partially explain the stronger correlation between training data and feedback valence, as utilizing only one control strategy would provide a more stable, consistent signal than when the subject attempts to utilize more than one.

In addition, given the characteristics of the detectable signal as illustrated in Figure 3.6, we find further evidence for a "satisfaction" signal underlying the active motor imagery. This demonstrates a measure that could be detected and utilized during active control of a BCI as a secondary measure of control. This could create more of an interactive bidirectional control loop, as the users are actively engaging and reacting to cursor movement, rather than merely observing cursor movement as an outcome of their motor imagery control. This has implications towards possibly improving system performance as well as increasing the number of users who can successfully use a BCI.

Here we have demonstrated the existence of an EEG correlate for loss of control and increased workload that manipulates the feature space of the motor imagery signal

during periods of positive and negative feedback. This signal has the potential to be utilized for the introduction of context awareness for BCI applications.

Future work will include investigating the nature of this feedback-related feature space manipulation. This could potentially lead to the ability to rotate the more negative valence feature space to that of the regions of more positive valence or to use a motor imagery feature space that is perpendicular to the space of changes invoked by differences in feedback valence, thus improving system performance.

This could also lead to user state detection for the improvement of ERD-based BCIs. It could be possible to identify when BCI users are entering a negative user state by a combination of identifying motor imagery feature space manipulation, relative shifts in C3/C4 lateralization, and changes in alpha and theta frequency bands. Identifying regions of negative shifts in user state could allow for modifying system performance to better suit the user.

3.6 Chapter Acknowledgement

The text of Chapter 3 is currently in the submission process for publication. The dissertation author is the primary author for this publication, titled “The effect of real-time positive and negative feedback on motor imagery performance”, revised and resubmitted for publication in *Frontiers in Human Neuroscience*.

Chapter 4

Utilizing user satisfaction as a control signal for an online BCI

4.1 Chapter Abstract

Here we investigate the possibility of an online BCI utilizing the user's dissatisfaction and satisfaction (DS system) signals as a principal control signal. We perform within- and between-subject comparisons between this system and a traditional motor imagery BCI using right- vs left-hand motor imagery (RL system) in order to demonstrate usability. Despite the user's active task for each paradigm being the same, the DS system outperforms the RL system for almost all subjects. In addition, these systems provide evidence in an online paradigm for the previously described feedback-related signals.

4.2 Introduction

There has been investigation into the use of user feedback signals as augmentation for motor imagery BCI systems. Specifically, error-related signals using both offline [43] and online [42] integration of error potentials into a motor-imagery based BCI. Artusi and colleagues utilize error detection in order to alter the BCI response after the entire trial is over, thus utilizing it as a post-hoc correction mechanism [42].

However, there are other useful feedback-related signals that could be used for a BCI system. For example, there has been work investigating the recognition of happy vs frustrated emotional states. Onton and Makeig have looked at the EEG-based recognition of different emotional states [49]. Emotion (both the associated valence and intensity) has also been recognized using other biosensors [85].

Previous research has also demonstrated distinct frontal lateralization in alpha power for positive and negative emotions (as evoked by the more relevant feat of internal generation, rather than from passive viewing of positive or negative stimuli) in frontal EEG [44, 45]. Left-lateralization increases in alpha (8-12Hz) power tend to correspond to positive emotions and right-lateralization for negative emotions. This lateralization could possibly indicate that spatial filtering, coupled with alpha (8-12Hz) and theta (4-7Hz) bandpower calculation can be very effective for the single-trial classification of emotions.

One critical issue in practical BCI use that may cause problems is the non-stationary nature of EEG signals [17]. EEG signals may change drastically from offline training to online use as well as during the actual experiment. This may occur due to mental state changes in the user, electrode movement or changes in skin conductance (such as from sweating). This drift can lead to a change in the optimal decision boundary between control classes, leading to loss of control of the BCI which leads to frustration and further drift of EEG signals from their training baselines [18]. Current solutions for control tend to focus on classifier adaptation, which necessitates re-training the classifier during the experiment [18, 17]. However, this does not entirely address the issue.

Addressing these issues requires a system that acts upon more natural control signals and is more robust towards pattern drift and user control. Professor de Sa has previously used an absorbing Markov chain to demonstrate the effectiveness of a paradigm that utilizes control signals associated with satisfaction and dissatisfaction as opposed to simple right vs left control. It was found that the information transfer rate (ITR) for both systems are equal when the classification boundaries are optimal; however the new system was more robust towards suboptimal classification boundaries. In terms of a real BCI system, these suboptimal classification boundaries could be the result of EEG non-stationarity. These results indicate that a system using dissatisfaction and satisfaction

control (DS) could be more effective for EEG-based BCI control than a traditional right vs left (RL) system [86].

Here we investigate the feasibility of such a system: an online BCI system controlled solely by the user's satisfaction with system performance. We compare its performance (both within and between subjects) to a traditional right vs left motor imagery BCI system.

4.3 Methods

4.3.1 Subjects

Five right-handed subjects (mean age = 27.4, one female) participated in the experiment. They signed an informed consent form after the study was approved by the University Institutional Review Board. All subjects were given verbal and written instructions prior to the experiment as to how to perform kinesthetic motor imagery. At the end of each block, the subject was instructed to rate the level of control they felt they had over the system from a scale of one to five, where one is no control and five is perfect control.

4.3.2 Experimental Setup

Data were recorded using a 64-channel BioSemi ActiveTwo system with a sampling frequency of 512 Hz, bilaterally referenced to the mastoids. In addition, EOG activity was recorded at the outer canthus and below the right eye in order to monitor eye movement. All EMG electrodes were also bilaterally referenced to the mastoids.

This particular system involves the control of a cursor moving left or right towards a white circular target, located at the left or right extreme of the screen. For each trial, a circular cursor started in the middle of the screen. After 2.4 seconds, the cursor starts to move in discrete movements to the right or to the left based on classifier output every 1.2 seconds. The trial ends when the right or left edge of the screen is reached or after 12 movements have been made. There is a 2 second inter-trial interval.

For this experiment, we compare two different control methods. These two

methods are traditional right vs left motor imagery (RL) and dissatisfaction vs satisfaction motor imagery and feedback signals (DS).

In order to control the system during RL blocks, the subject was instructed to utilize kinesthetic motor imagery to imagine drumming the fingers on their right hand to move the cursor towards a right target, and drumming the fingers on their left hand to move the cursor towards a left target. In order to help differentiate between blocks, for this control method the controlled cursor is red.

For DS blocks, the control system involves identical motor imagery. However, the context is different from the control scheme for RL blocks. At the beginning of each trial, the cursor moves, with random probability, to the left or to the right. The subject then uses kinesthetic motor imagery of the right hand to keep the cursor moving in the correct direction, and their left hand to change direction when it is moving in the incorrect direction. This control scheme generates a more interactive method to control the BCI system, as it requires the subject to integrate their active task with the feedback they are receiving.

For the DS control method, the cursor is colored blue. In addition, the classifier incorporates information from satisfaction signals (as described below) in addition to motor imagery. Since the active motor imagery task requires the subject to actively engage the system feedback, we utilize the additional information by using additional classifiers associated with system "satisfaction". During the "helped" trials, perturbation (as defined below) occurs on the combined classifier results from all features.

The experiment consisted of 5 blocks of 20 trials for both DS and RL control, for a total of 10 blocks. Block order was randomly determined prior to the experiment. In addition, in order to avoid issues with training subjects on data with disparate visual feedback [27], the users had no control over the first block for each method, and were given partial control over the next block for each method until gaining complete control for the last three blocks of each method. The early "helped" trials (during Block 2 of each method) were conducted by perturbing the classifier output probability by a factor of 0.5 towards the known "correct" output. The equation is given below:

$$p_{new} = p + 0.5 * C \tag{4.1}$$

Where p is the modified classifier output probability (scaled from its original range of [0 1] to [-1 1]), C is “-1" for class 1 and “1" for class 2 and p_{new} represents the perturbed classifier output probability.

Separate classifiers were trained for the RL and DS methods. After each block, the respective classifiers were re-trained on the last 200 windows from that method in order to adapt to the changing motor imagery feature space [76].

4.3.3 Data Analysis

Pre-processing

For online classification, no pre-processing was applied. However, trial rejection was performed during classifier training after each block in order to ensure classifier quality.

Trial rejection and artifact removal was applied for later offline analysis. This consisted of high-pass filtering the collected data at 1 Hz using an FIR filter, then segmenting it into 10 second chunks (spanning the entire length of the trial) and visually inspecting for trials with excess movement artifacts (as characterized by variance from the mean data probability distribution and increase in absolute voltage). Trials with excess movement artifacts were subsequently removed. Excess voltage changes were characterized as those above 1000 μV, and high variance trials were characterized as those that varied by more than 5 standard deviations from the mean distribution. This artifact rejection was performed using the EEGLAB package distributed by the Swartz Center for Computational Neuroscience (SCCN) [59].

In addition to visual inspection, Independent Component Analysis (ICA) was used to reject data artifacts. Infomax ICA [60] was trained on the epoched and filtered datasets, and the resulting artifactual components associated with muscle movements were removed based on source location and spectral patterns.

Feature extraction for motor imagery

Spatially dependent power decrease in mu (8-13Hz) and beta (14-25Hz) frequency bands has been observed during movement, prior to movement and during imag-

ined or covert movement [14]. This has been used as a feature to drive commands in motor imagery and intended movement-based BCI experiments. In order to enhance this frequency information, we use common spatial patterns (CSPs) [61] to find a set of filters that maximize the projected variance (power) for one class while minimizing it for the other class. Applying CSPs to band-pass filtered signals emphasizes the spatially-segregated power decrease differences between the different classes [61].

All classification for motor imagery and satisfaction/dissatisfaction signals was performed on 1s chunks of data (from -0.25s to 0.75s after each cursor movement). Feature extraction for motor imagery was conducted by band-pass filtering (with a FIR filter) the data from 7-30Hz, then using three regularized CSPs [62] for each class (total 6) [61] to provide the feature set for the classifier, linear discriminant analysis (LDA)[63]. Post-hoc offline classifier performance was validated using 10-fold cross validation, and success rate was calculated based on the number of correct versus incorrect classifications for each trial.

Feature extraction for dissatisfaction/satisfaction

For online RL control, only motor imagery was considered. For online DS control, we combined feature extraction for motor imagery with feature extraction to detect the feedback response signal, which involves the combination of three additional features [64]. These features were chosen based on previous studies implicating spatial activity in the theta and alpha bands [73, 72] for frustration and increased workload, as well as studies motivating the detection of error potentials [41].

Separate LDA classifiers were trained for all features. The utilized features include both the time-domain (the channel activity) and spectral activity (as given by the average power over the particular frequency band and time period) at electrode FCz, as well as CSPs for several frequency bands. All feature extraction was performed on the same 1s window of data as the motor imagery feature. We used a total of four features, selected based on performance with previously collected pilot data from separate, informed subjects:

A Regularized CSPs for motor imagery, implemented as described above.

B Regularized CSPs for satisfaction signals, bandpassed from 4-25Hz, as described in Chapter 3.

C Spectral power at FCz from 1-10Hz after being spatially filtered using a large Laplacian filter. The large Laplacian filter around FCz subtracts 0.25 of each of the values at electrodes CPz, FC4, FC3 and AFz from the value at FCz.

D Pattern matching at electrode FCz [87], consisting of averaging each non-overlapping 50ms of data, for a total of 20 bins.

These features were combined by averaging the LDA output probabilities together in order to arrive at a classification decision.

In order to determine classifier significance for both methods, we fit the accumulated values to a binomial distribution (with an N equal to the total number of trials), then compared to a classifier that would perform at random chance, as described in [67].

4.4 Results

4.4.1 Online Performance

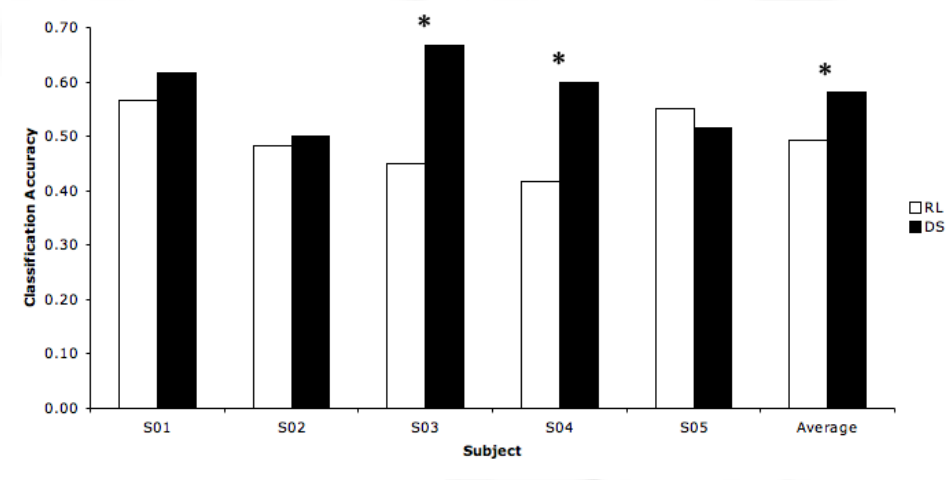


Figure 4.1: Target hit rate for each method across subjects during online performance for unaided blocks. DS results include satisfaction signals as detailed in “Data Analysis".

The comparison of online performance between the DS and RL systems demonstrates a slight advantage for the DS system. Target hit rate represents the success of

each subject to move the cursor to the target within the allotted time for each trial. As demonstrated in Figure 4.1, 3 of 5 subjects performed comparably for both RL and DS systems, while 2 subjects performed significantly better ($p<0.05$) for the DS system.

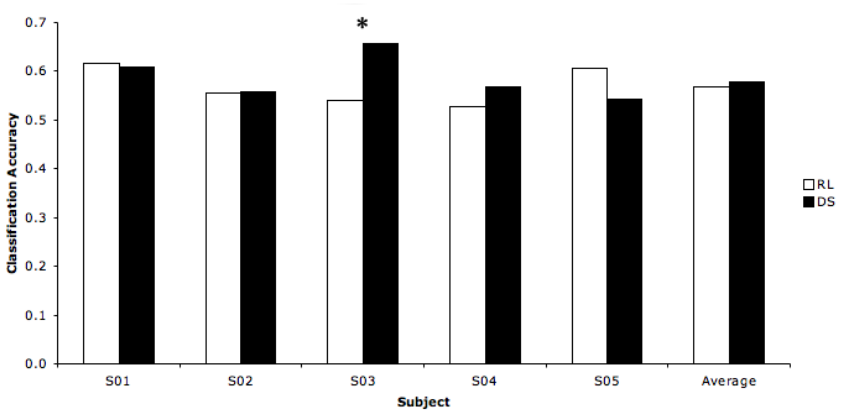


Figure 4.2: Classification rate for each method across subjects during online performance for aided and unaided blocks. DS results include satisfaction signals as detailed in “Data Analysis".

Online classification performance of individual windows was more equal between the two systems, with only one subject performing significantly better for the DS system than the RL system. Figure 4.2 illustrates this similarity. It’s significant to note that despite similar classification accuracy, the target hit rate for the DS system is stronger than for the RL system.

User-reported satisfaction also demonstrated a preference for the DS system, as seen in Table 4.1. Preference was gathered for S1-S4 and S6 (as S5 is the author), and was positively correlated with both online system accuracy (correlation coefficients were 0.685 for RL and 0.696 for DS) and online system target hit rate (0.766 for RL and 0.678 for DS).

Table 4.1: Subject-reported satisfaction with online BCI performance during controlled blocks.

	S1	S2	S3	S4	S6	Average
RL	3.88	2.63	2.50	2.38	3.25	2.93
DS	3.67	3.00	2.63	3.00	4.15	3.29

In order to get a complete picture of system performance, we need to incorporate both classification accuracy and the number of steps required to reach a decision. The information transfer rate (ITR) is a useful measure that takes both of these factors into account [66].

When looking at the ITR for each control method, we find that the DS method has the advantage over the RL method for 4 of 5 subjects, as illustrated in Figure 4.3. These differences are not significant on a subject by subject basis, however when all subjects are considered together, DS holds a significantly ($p<0.01$) stronger ITR.

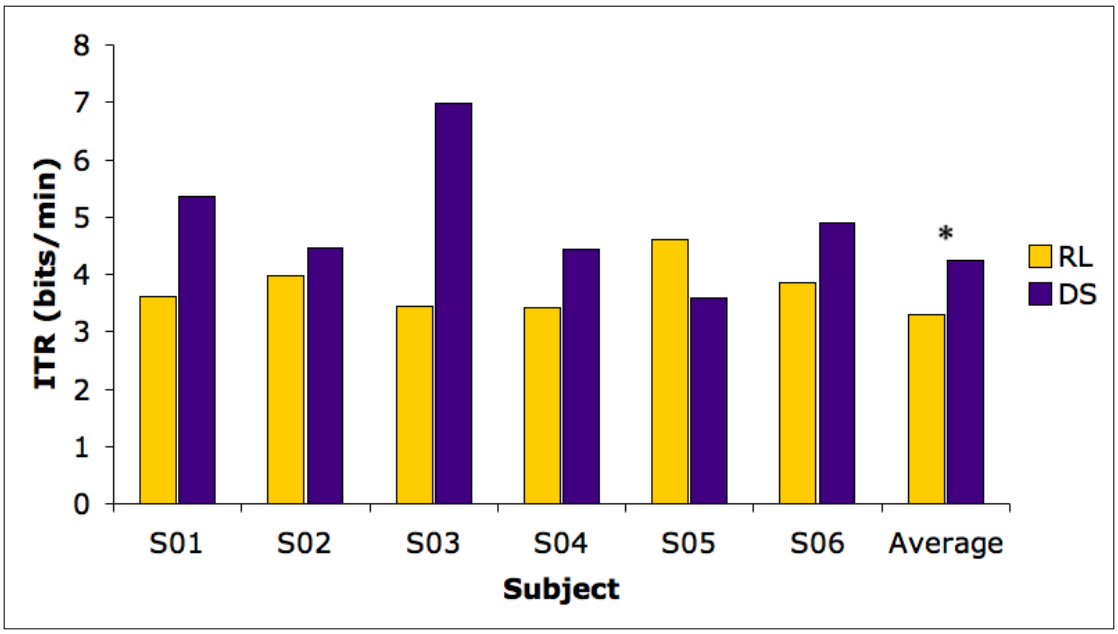


Figure 4.3: Online ITR for each method during controlled blocks in bits/min. Note that DS results include satisfaction signals as outlined in “Data Analysis".

Given the system-aided nature of the first two blocks, it is expected that initial online performance is impressive, and tails off when subjects are given complete control for blocks 3, 4, and 5 for each method. However, classification accuracy and system hit rate both remain significantly above chance ($p<0.05$) for all subjects.

4.4.2 Offline Classification Analysis

In order to properly parse out the aspects of the signal that correspond with greater performance for DS over RL, we need to perform post-hoc analysis for each of

the relevant signals.

When the data is pre-processed by performing artifact and trial rejection, post-hoc offline classification was still significantly better than chance for at least one method for each subject. For offline analysis, the comparative performance observed in the online system holds. The DS system was more effective overall than the RL system. This indicates that system performance during online performance is not reliant on motor artifacts for classification accuracy.

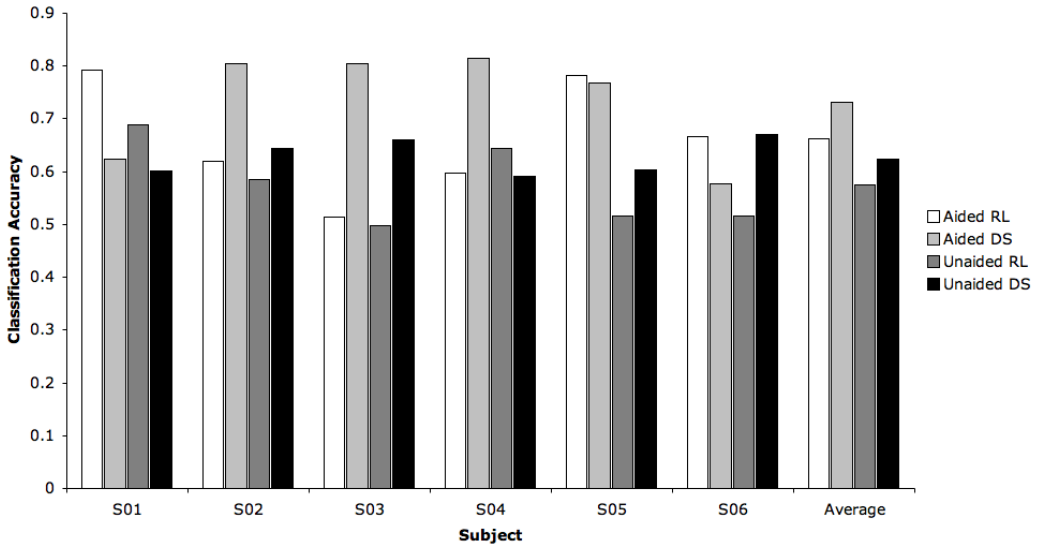


Figure 4.4: Post-hoc offline motor imagery classification accuracy with data pre-processing. Notice that aided blocks generally have better performance than unaided blocks.

In addition, as can be seen in Figure 4.4, four of five subjects receive better offline classification rates for the DS system than for the RL system (with both systems using motor imagery alone), indicating that it represents a more reliable overall control signal. In addition, as was observed in Chapter 3, motor imagery performance during aided blocks (where subjects were presented favorable visual feedback), outperformed unaided blocks (where visual feedback is not necessarily positive, dependent on subject performance). Five of six subjects for both the RL method and the DS method have better post-hoc offline motor imagery performance during aided blocks than during unaided blocks. This may be due to differences in visual feedback as previously found, or it could be the result of user fatigue during the latter portion of the experiment.

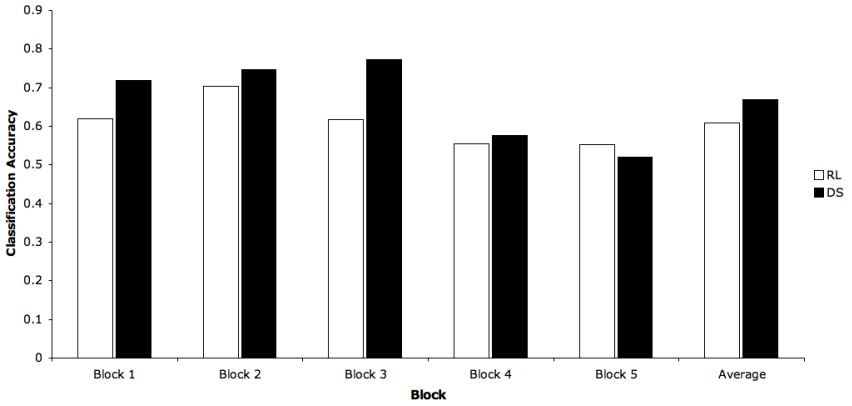


Figure 4.5: Post-hoc offline motor imagery classification accuracy validated with 10-fold cross validation.

As these motor imagery classification results are calculated using 10-fold cross-validation across the entire data set, this could indicate that the DS system provides a more stable, consistent motor imagery signal. However, based on cross-validation results from motor imagery classification within each block (as seen in Figure 4.5), it is evident that the DS system does not outperform the RL system on a block-by-block basis.

4.4.3 Distinguishing between methods

Given the disparity in results, it was necessary to ensure that the users were performing the same task for both RL and DS control schemes.

Each classification window was re-labeled as its control type, trial order was randomized, classes were balanced, and feature extraction (CSPs on data bandpassed from 4-12Hz) was performed on the original classification windows from RL and DS control schemes. Results were validated using cross-validation across the whole dataset. The same motor imagery classifier previously used for classifying right vs left was used for this analysis. However, we were unable to discriminate between these control methods with greater performance than chance, as can be seen in Table 4.2.

This indicates that any differences in performance are not due to changes in motor imagery techniques for each method, but rather some aspect of the control scheme itself. Furthermore, since both methods utilize the same motor imagery, it is possible to

Table 4.2: Post-hoc offline classification accuracy discriminating between DS vs RL methods.

	Accuracy
S01	0.476
S02	0.488
S03	0.537
S04	0.523
S05	0.463
S06	0.516
Average	0.497

use one data set as the training set for the other. In fact, this analysis results in both systems classifying above chance for four of five subjects. Table 4.3 demonstrates how the classification accuracy for each control type changes for whole data cross-validation, leave-one-block-out cross-validation, and when training a classifier on the data of the opposite control type. As can be seen, all techniques perform similarly across each cross-validation type, with the exception of whole-data cross-validation for the DS system. This provides further evidence that the motor imagery performance is in the same feature space for both methodologies, and any differences in performances are the consequences of control scheme and user satisfaction.

Table 4.3: Post-hoc offline motor imagery classification accuracy when trained on the opposing method (DS on RL, RL on DS), blockwise cross-validated and over the whole data.

	Whole Data		Blockwise		Other Method	
	RL	DS	RL	DS	Tested on RL	Tested on DS
S01	0.559	0.651	0.570	0.552	0.565	0.550
S02	0.488	0.610	0.549	0.554	0.580	0.568
S03	0.684	0.723	0.558	0.560	0.577	0.588
S04	0.490	0.704	0.556	0.583	0.562	0.539
S05	0.626	0.779	0.584	0.533	0.542	0.551
S06	0.649	0.671	0.571	0.655	0.557	0.614
Average	0.577	0.703	0.565	0.573	0.564	0.568

4.4.4 Evaluation of satisfaction signal

One characteristic of this experiment is that early blocks (with more successful visual feedback) typically have more effective post-hoc offline results. This may be due to user fatigue, in addition to having more positive feedback (as was demonstrated in Chapter 3). These results can be seen in Figure 4.5, where it is evident that classification accuracy generally decreases towards the end of the experiment.

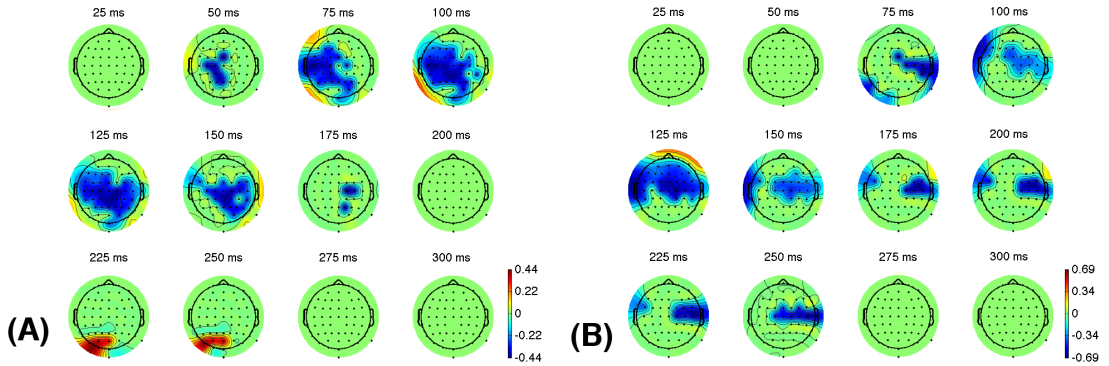


Figure 4.6: Grand average scalp maps for the difference in theta (A) and alpha (B) band power between good/early and bad/late blocks for the **DS method**. These figures demonstrate a strong difference in both theta and alpha power over the centro-parietal region 75-200ms after each cursor movement.

The spectral properties of good/early and bad/late blocks also reveal differences between the two control methods. This is consistent with our findings in Chapter 3, however in this particular instance it is very difficult to separate out what portion of this effect is due to temporal factors and what portion is due to mental correlates of “loss of control". Overall theta and alpha patterns match with the offline results from Chapter 3, but RL seems to be much more susceptible to differences between good/early and bad/late blocks. This is apparent in a comparison between Figures 4.6 and 4.7. There is a much greater difference in statistically significant ($p<0.05$) power calculations between good/early and bad/late blocks in the frontal areas for the RL method, possibly indicating a greater level of fatigue or strain for the RL method than for the DS method. In addition, differences in response peaks earlier for the DS method than the responses for the RL method. Significance for the spectral scalp maps was determined using a paired t-test at each time point across all trials and subjects.

Although these spectral results are not corrected for multiple comparisons (given the multiple channels and time points), the pattern consistency over time indicates that they would likely remain significant when provided for multiple comparisons. In addition, given that the different data points are likely correlated, the Bonferroni method may prove to be overly conservative, and cluster analysis would be the better option. These results are presented for illustration, and not as a significant marker of neural activity.

For the purposes of this study, we chose not to integrate our findings from Chapter 3 (where we demonstrate the manipulation of the motor imagery feature space by feedback valence) into this experiment for several reasons. The design of this study makes it very difficult to properly isolate the effects of satisfaction with system performance from the differences in EEG responses due to temporal factors. In addition, given that this study already investigates the comparison between two control methods, it was determined that adding in an additional variable would only generate confusion.

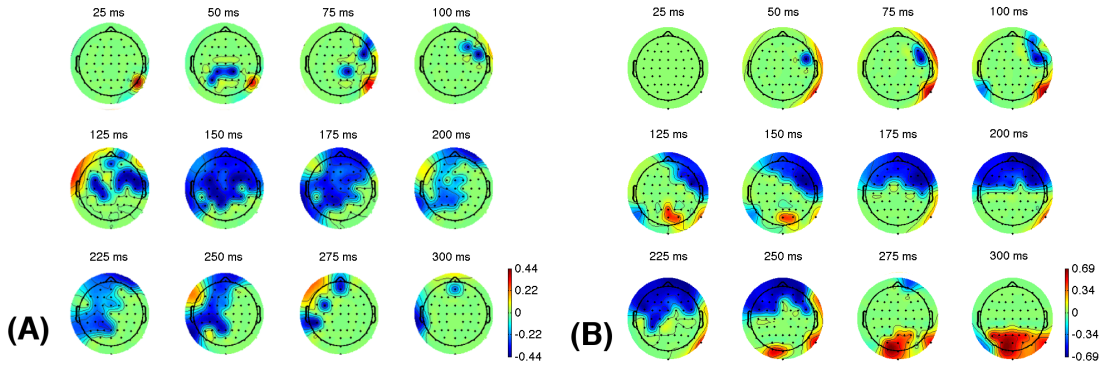


Figure 4.7: Grand average scalp maps for the difference in theta (A) and alpha (B) band power between early/positive and late/negative blocks for the **RL method**. These figures demonstrate a strong difference in both theta and alpha power over the centro-parietal region 100-250ms after each cursor movement.

The feedback-related satisfaction signals utilized in the DS system for classification (specifically CSPs on data bandpass filtered from 4-25Hz) can also be classified accurately in the RL system. Data were preprocessed as described above and classifier efficacy was determined using 10-fold cross-validation across the whole data set on the same windows used for motor imagery classification. Results can be found in Table 4.4. Note that classification accuracies across most subjects are not significantly different between control schemes, indicating that this can be a useable signal even in RL systems.

In addition, it is evident that for most subjects, using CSPs as opposed to electrode FCz is more effective for identifying these signals.

Table 4.4: Post-hoc offline classification accuracy for positive versus negative cursor movements. All results are statistically significant ($p<0.01$). Each letter feature corresponds with the features from “Data Analysis".

	DS					RL				
	Overall	A	B	C	D	**Overall**	A	B	C	D
S01	**0.685**	0.677	0.690	0.569	0.552	**0.685**	0.707	0.698	0.628	0.579
S02	**0.690**	0.585	0.660	0.585	0.510	**0.660**	0.597	0.653	0.597	0.549
S03	**0.737**	0.764	0.737	0.581	0.622	**0.651**	0.694	0.629	0.529	0.571
S04	**0.688**	0.719	0.727	0.615	0.604	**0.636**	0.616	0.663	0.535	0.531
S05	**0.821**	0.813	0.830	0.665	0.589	**0.586**	0.667	0.603	0.521	0.496
S06	**0.639**	0.684	0.665	0.690	0.709	**0.683**	0.683	0.700	0.574	0.530
Average	**0.723**	0.707	0.718	0.618	0.598	**0.652**	0.661	0.658	0.564	0.543

4.4.5 Evaluation of error signal

We also evaluated the differences between user responses to steady-state and change-in-direction cursor movements in an online setting in order to appropriately follow up the results from Chapter 2. In addition, given the more interactive nature of the DS system, the effect of this control scheme on user responses to cursor movements is an important factor to consider.

Table 4.5: Post-hoc offline classification accuracy for positive versus negative changes in direction. All results are statistically significant ($p<0.01$). Each letter feature corresponds with the features from “Data Analysis".

	DS					RL				
	Overall	A	B	C	D	**Overall**	A	B	C	D
S01	**0.689**	0.635	0.649	0.662	0.649	**0.660**	0.612	0.633	0.601	0.590
S02	**0.705**	0.614	0.614	0.602	0.546	**0.708**	0.583	0.569	0.653	0.639
S03	**0.862**	0.845	0.776	0.603	0.621	**0.570**	0.553	0.483	0.544	0.509
S04	**0.754**	0.659	0.627	0.627	0.651	**0.636**	0.466	0.458	0.542	0.500
S05	**0.860**	0.787	0.827	0.660	0.587	**0.710**	0.565	0.645	0.565	0.516
S06	**0.921**	0.684	0.842	0.632	0.526	**0.573**	0.458	0.479	0.563	0.583
Average	**0.792**	0.704	0.722	0.631	0.596	**0.643**	0.539	0.544	0.578	0.556

In addition to the findings illustrated in Table 4.4, we found that for 2 subjects for RL and for 5 subjects for DS, the differences during changes in direction are even more discriminable than those for cursor movements in the same direction. Post-hoc classification results for changes in direction can be found in Table 4.5; this classification was performed as described in Chapter 2. Comparing Tables 4.4 and 4.5 demonstrates that activity at electrode FCz can be more predictive than CSPs, particularly for the RL method.

On average, there were $170.7+/-42.4$ changes in direction per subject for the DS method, and $142.5+/-39.8$ changes in direction per subject for the RL method.

These findings provide online confirmation for our findings for RL control from the offline experiment outlined in Chapter 2. The temporal activity during incorrect movements are similar as well. As can be seen in Figure 4.8, in addition to the feedback related negativity at around 200ms, we also notice a depressed P3 response that is consistent with increased workload [73]. In addition, when comparing the differences between Figure 4.8A and B, notice that not only are the ERP patterns much more similar for correct and incorrect movements without considering of changes of direction, but that the regions of significant difference ($p<0.05$, indicated by shading) are smaller.

There are also major differences when comparing the change in direction and steady state ERPs for the RL system and the DS system. These differences are likely due to the fact that the DS system causes the user to directly engage this feedback signal as a control mechanism. This causes issues during a change in direction, when regardless of a 'correct' or 'incorrect' change, the user must change their motor imagery action, resulting in a less distinguishable ERP trace. This is apparent when noting that the regions of significant difference are larger in Figure 4.9B than in Figure 4.9A.

Interestingly, this ERP difference between RL and DS is most prevalent during incorrect movements (as seen in Figure 4.10. Incorrect movements (regardless of whether they are a change in direction) during RL control result in a stronger P3 amplitude reduction than during DS control, while correct movements are unaffected. This is even true during a change in direction, which is unexpected since a change in direction requires the user to change motor imagery for the DS system. This should affect the ERP trace regardless of whether the change is correct or incorrect, however the correct

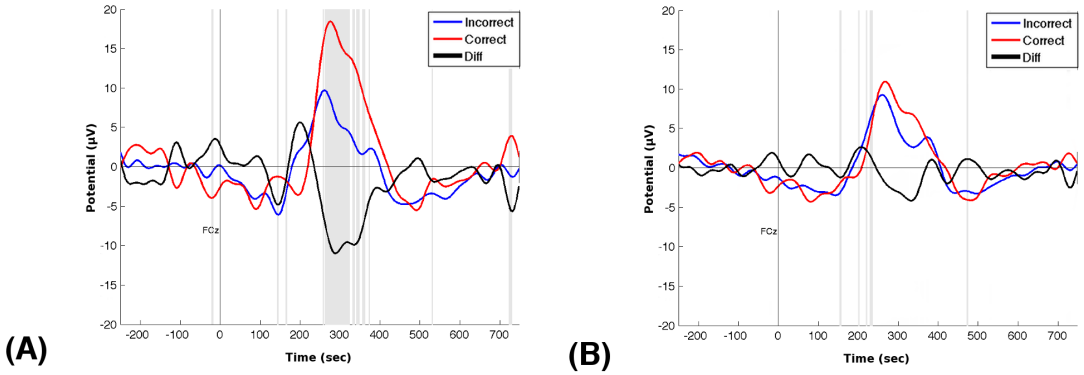


Figure 4.8: **A:** Grand average trace of the ERPs, lowpassed at 20Hz, at electrode FCz associated with cursor changes in direction for the *RL method*. Correct change in direction demonstrates a markedly different trace from an incorrect change, which possibly indicates the same complex as a correct change in direction coupled with a clear negative error potential (Ne). This is coupled with a subsequent decreased P3 response, consistent with increased workload. **B:** Grand average trace of the ERPs at electrode FCz associated with positive and negative cursor movements (not necessarily a change in direction). Note that the error potential is not as pronounced, and differences in P3 amplitude are not as pronounced as in A. Shaded areas for both A and B indicate regions of statistically significant difference ($p<0.05$).

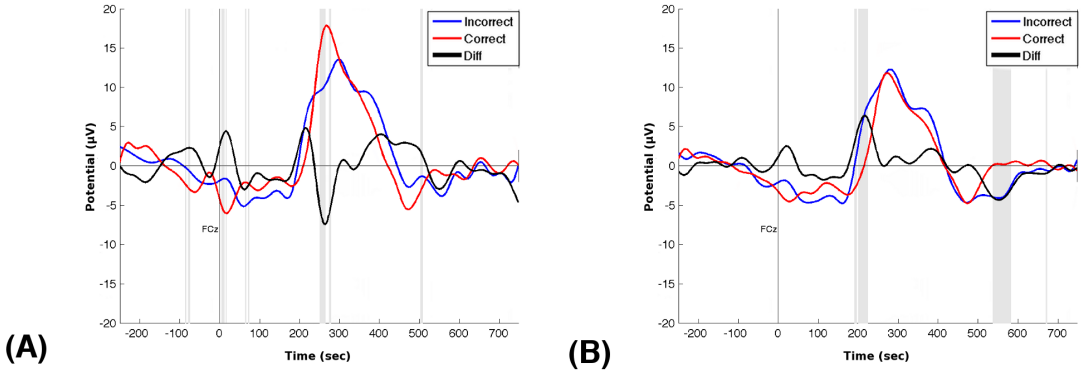


Figure 4.9: **A:** Grand average trace of the ERPs, lowpassed at 20Hz, at electrode FCz associated with cursor changes in direction for the *DS method*. Note that the error potential is not nearly as pronounced as in Figure 4.8. This is coupled with a subsequent significantly decreased P3 response, consistent with increased workload. **B:** Grand average trace of the ERPs at electrode FCz associated with positive and negative cursor movements (not necessarily a change in direction). Shaded areas for both A and B indicate regions of statistically significant difference ($p<0.05$).

changes appear to be largely unaffected.

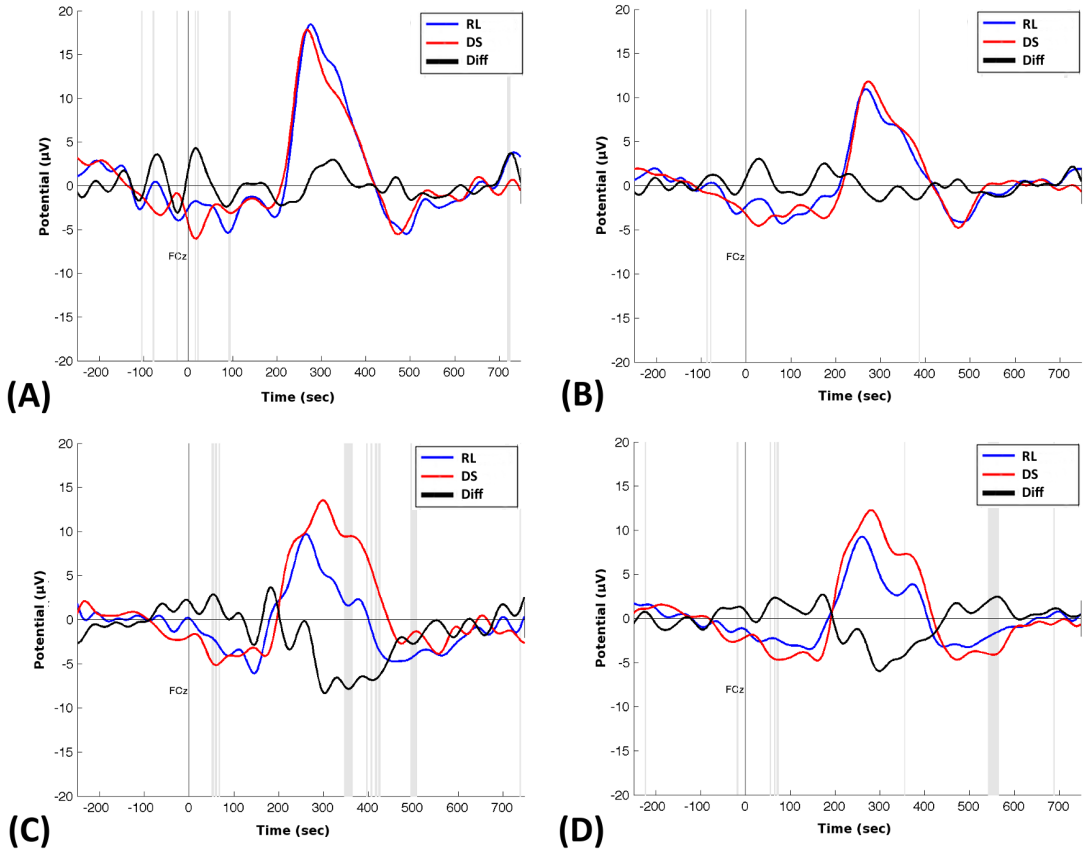


Figure 4.10: **A:** Grand average trace of the ERPs, lowpassed at 20Hz, at electrode FCz associated with correct cursor changes in direction, **B:** correct cursor movements (not necessarily a change in direction), **C:** incorrect cursor changes in direction, and **D:** incorrect cursor movements (not necessarily a change in direction). Shaded areas for all figures indicate regions of statistically significant difference ($p<0.05$). Note that incorrect movements demonstrate the largest differences between methods, while correct movements result in very similar responses.

It is important to note that there are strong differences in the ERP traces associated with changes and steady state cursor movement. In both contexts (and for both methods), the principal regions of difference are represented by the P3 response to cursor movements. However, for changes in direction this difference is primarily in the ERP amplitude, while for non-changes the difference is in P3 onset.

4.5 Discussion

Here we have demonstrated a novel system for utilizing user satisfaction as a control signal for a BCI. These results demonstrate that for most subjects, it performs comparably to traditional motor imagery controlled systems. However, for some subjects there is a significant increase in system performance brought on by the integration of user satisfaction signals. In addition, differences in spectral activity could possibly indicate that users experience more fatigue or workload when using the traditional RL method than when using the DS method. This is further borne out in the comparison for user control ratings for each method, as users exhibited a slight preference for the DS method.

This study has also validated our previous, offline work on error potentials and other feedback-related signals. Not only are these signals utilized effectively for control with the DS method, but they are still present and classifiable when not an explicit part of user instructions. This provides great implications for the importance of closed-loop control in future BCI applications.

These results could contribute to improving the global usability of BCIs. If we can find a more natural way to control these systems, we can improve their utility and broaden their scope. This method of utilizing feedback-related signals is only one method for closed-loop BCI control. Instead of explicitly utilizing feedback-related signals for control (as in the DS system described here), it may be possible to instead augment RL performance (or any other paradigm). This could be done by utilizing error correction for identifying correct and incorrect changes in direction or local satisfaction signals (as detailed in Table 4.4) in order to immediately change or alter the system output.

This could also be achieved on a more global scale, by utilizing the underlying workload/loss of control signal (as identified in Chapter 3) in order to affect how the entire system interprets user signals. This could take the form of altering feature weights or the feature space according to whether the system detects that the subject is feeling frustrated or experiencing a loss of control. This could provide a highly effective method for both improving global usability of BCIs, and helping to compensate for user fatigue and changing mental state.

4.6 Chapter Acknowledgement

Chapter 4 is currently being prepared for publication.

Chapter 5

Contribution of Work

Our work as described in this dissertation makes the following contributions to the field of brain-computer interfaces:

- We propose a novel method of integrating feedback-related potentials into an online BCI, which takes advantage of varying step sizes and differences in classifier confidence.

Current work on error correction typically treats user responses to cursor movements the same regardless of whether that response was to a change in direction or not. In addition, current studies only utilize these feedback-related signals as error correction mechanisms. We established that the user response to cursor changes in direction during a brain-computer interface are different than those associated with a constant direction. Moreover, we found that treating these feedback-related signals differently and integrating them better into the control scheme results in a system that can improve upon the performance of brain-computer interfaces with error correction. Furthermore, classifiers for error correction can be more or less confident about error recognition, and utilizing a system that uses probabilistic combination (as for motor imagery) can make better use of this information than current methods where the error detection always overrides motor imagery.

- The properties of real-time EEG associated with varying visual feedback during online BCI control are explored and elicited.

In addition to the differential user response to changes in direction and steady-state direction, we also noted that both signals were discriminable. In addition, there is a noticeable “global satisfaction" signal in the theta (4-7Hz) and alpha (8-13Hz) bands that is characterized by the increase in power over the centro-parietal regions during periods of negative feedback. This is consistent with previous literature describing increased workload and the sensation of a loss of control [73]. This is unique, as it is the first time this signal has been characterized and related back to increased workload during motor imagery tasks. Previous work on workload measurement has been in the form of n-back tasks or on induced frustration during tasks executed by button presses.

- We investigate the effect of these feedback-related signals on task performance. These effects occur even when the presented feedback has no relation to actual motor imagery performance.

- We also note that differences in motor imagery performance due to difference in visual feedback are due to a manipulation of the motor imagery feature space, rather than motor imagery consistency as originally hypothesized.

Moreover, this global “satisfaction” signal has an effect on subject motor imagery performance. Providing more positive feedback induces stronger motor imagery, while more negative feedback induces weaker motor imagery. This feedback-induced difference in motor imagery appears to generate stronger trained classifiers, which we hypothesized would indicate that positive feedback should be presented to subjects during training in order to induce stronger training data.

However, contrary to our hypothesis and established work, we found that this difference in motor imagery performance appears to be caused by a manipulation of the feature space, rather than simply being the result of an improved and more consistent training signal. This provides an important understanding of the nature of global “dissatisfaction” signals. If we can discover the way in which these signals manipulate the feature space, it may be possible to readjust the feature space, thus rescuing BCI performance during periods of frustration brought on by negative feedback. This would provide valuable insight into how to rescue motor imagery performance when users are in a negative mental state.

- We present an interactive online BCI based around interaction with visual feedback. We compare this system to a traditional motor imagery-based BCI and demonstrate that it is a viable method of control.

- We provide evidence for the utility of feedback-related signals in an online BCI system.

We also demonstrate an online BCI system that allows the user to interactively control a cursor on the screen by using motor imagery to indicate user satisfaction as opposed to indicating direction. This system, as hypothesized, seems to be more robust to EEG non-stationarity than normal directionality-based systems. User control is improved, and this demonstrates that local feedback signals are useful for effectively controlling a BCI. This provides a valuable starting point for investigating novel methods of BCI control.

In an online system, when changes in direction are not controlled, we still notice a difference between user response to changes in direction and steady-state directions. The spatial and temporal actions are distinct, and indicate that systems may benefit from training unique classifiers for changes in direction and for non-changes. In addition, global and local satisfaction signals as initially identified during offline systems (where users have no control) remain discriminable. This moves beyond current work that focuses on error correction as a method of integrating user feedback into BCI control.

Taken together, these contributions indicate that motor imagery BCI systems are effectively improved by tightly integrating feedback-related signals into control. We demonstrate in an online system one method for integrating feedback into motor imagery-based BCIs, while uncovering several other signals that may benefit from being used in unique ways to improve BCI systems.

Future work will focus on new methods for integrating these feedback-related signals even more into BCI systems, as well as the possible expansion beyond one-dimensional control.

Bibliography

[1] Ramesh Srinivasan. Methods to improve the spatial resolution of EEG. *International Journal of Bioelectromagnetism*, 1(1):102–111, 1999.

[2] A Schlögl, C Neuper, and G Pfurtscheller. Estimating the mutual information of an EEG-based brain-computer interface. *Biomedizinische Technik/Biomedical Engineering*, 47(1-2):3–8, 2002.

[3] Tzyy-Ping Jung, Scott Makeig, Colin Humphries, Te-Won Lee, Martin J Mckeown, Vicente Iragui, and Terrence J Sejnowski. Removing electroencephalographic artifacts by blind source separation. *Psychophysiology*, 37(2):163–178, 2000.

[4] John Polich. Updating P300: an integrative theory of P3a and P3b. *Clinical neurophysiology*, 118(10):2128–2148, 2007.

[5] Samuel Sutton, Margery Braren, Joseph Zubin, and ER John. Evoked-potential correlates of stimulus uncertainty. *Science*, 150(3700):1187–1188, 1965.

[6] Francesco Piccione, Flavio Giorgi, P Tonin, K Priftis, S Giove, S Silvoni, G Palmas, and F Beverina. P300-based brain computer interface: reliability and performance in healthy and paralysed participants. *Clinical neurophysiology*, 117(3):531–537, 2006.

[7] Lawrence Ashley Farwell and Emanuel Donchin. Talking off the top of your head: toward a mental prosthesis utilizing event-related brain potentials. *Electroencephalography and clinical Neurophysiology*, 70(6):510–523, 1988.

[8] Emanuel Donchin, Kevin M Spencer, and Ranjith Wijesinghe. The mental prosthesis: assessing the speed of a P300-based brain-computer interface. *IEEE Trans. Rehabil. Eng.*, 8(2):174–179, 2000.

[9] Fabrizio Beverina, Giorgio Palmas, Stefano Silvoni, Francesco Piccione, and Silvio Giove. User adaptive bcis: Ssvep and p300 based interfaces. *PsychNology Journal*, 1(4):331–354, 2003.

[10] Pablo F Diez, Vicente A Mut, Enrique M Avila Perona, and Eric Laciar Leber. Asynchronous bci control using high-frequency ssvep. *J Neuroengineering and Rehabilitation*, 8(1):39, 2011.

[11] C Brunner, BZ Allison, C Altstätter, and C Neuper. A comparison of three brain–computer interfaces based on event-related desynchronization, steady state visual evoked potentials, or a hybrid approach using both signals. *J Neural Eng.*, 8(2):025010, 2011.

[12] J. R. Wolpaw. Control of a two-dimensional movement signal by a noninvasive brain-computer interface in humans. *Proc. of the Nat. Academy of Sciences*, 101(51):17849–17854, Dec 2004.

[13] J. A. Pineda, B. Z. Allison, and A. Vankov. The effects of self-movement, observation, and imagination on mu rhythms and readiness potentials (RPs): Toward a brain-computer interface (BCI). *IEEE Trans. Neural Syst. Rehabil. Eng.*, 8(2):219–222, Jun 2000.

[14] G. Pfurtscheller, C. Brunner, A. Schlögl, and F.H. Lopes da Silva. Mu rhythm (de)synchonization and EEG single-trial classification of different motor imagery tasks. *Neuroimage*, 31:153–159, 2006.

[15] Paul S. Hammon. *Adaptive Online Brain-Computer Interface for Interpretation and Visualization of Desired Reach*. PhD thesis, Department of Electrical and Computer Engineering, University of California, San Diego, 2009.

[16] C. Guger, G. Edlinger, W. Harkam, I. Niedermayer, and G. Pfurtscheller. How many people are able to operate an EEG-based brain-computer interface (BCI)? *IEEE Trans. Neural Syst. Rehabil. Eng.*, 11(2):145 –147, june 2003.

[17] P. Shenoy, M. Krauledat, B. Blankertz, R.P.N. Rao, and K-R. Müller. Towards adaptive classification for BCI. *J. Neural Eng.*, 3:R13–R23, 2006.

[18] *Towards an heuristic-based approach detecting nonstationarities in BCI features*, 2010. Abstract presented at BCI 2010.

[19] A Kübler, VK Mushahwar, Leigh R Hochberg, and John P Donoghue. Bci meeting 2005-workshop on clinical issues and applications. *IEEE Trans. Neural Syst. Rehabil. Eng.*, 14(2):131–134, 2006.

[20] D.J. McFarland, L.M. McCane, and J.R. Wolpaw. EEG-based communication and control: short-term role of feedback. *IEEE Trans. Rehabil. Eng.*, 6(1):7 –11, mar 1998.

[21] C Güger, G Edlinger, W Harkam, I Niedermayer, and G Pfurtscheller. How many people are able to operate an EEG-based brain-computer interface (BCI)? *IEEE Trans. Neural Syst. Rehabil. Eng.*, 11(2):145–147, 2003.

[22] Brendan Allison, Thorsten Luth, Diana Valbuena, Amir Teymourian, Ivan Volosyak, and Axel Graser. BCI demographics: How many (and what kinds of) people can use an SSVEP BCI? *IEEE Trans. Neural Syst. Rehabil. Eng.*, 18(2):107–116, 2010.

[23] Eleanor A Curran and Maria J Stokes. Learning to control brain activity: a review of the production and control of EEG components for driving brain–computer interface (BCI) systems. *Brain and Cognition*, 51(3):326–336, 2003.

[24] Christa Neuper, Reinhold Scherer, Selina Wriessnegger, and Gert Pfurtscheller. Motor imagery and action observation: modulation of sensorimotor brain rhythms during mental control of a brain–computer interface. *Clinical Neurophysiology*, 120(2):239–247, 2009.

[25] Y. Lee, J. Kim, S. Lee, and M. Lee. Characteristics of motor imagery based EEG-brain computer interface using combined cue and neuro-feedback. In *Engineering in Medicine and Biology Society (EMBC), 2010 Annual International Conference of the IEEE*, pages 4238–4241. IEEE, 2010.

[26] Aniruddha Chatterjee, Vikram Aggarwal, Ander Ramos, Soumyadipta Acharya, and Nitish V Thakor. A brain-computer interface with vibrotactile biofeedback for haptic information. *Journal of NeuroEngineering and Rehabilitation*, 4:40, 2007.

[27] Haihong Zhang, Sidath Ravindra Liyanage, Chuanchu Wang, and Cuntai Guan. Learning from feedback training data at a self-paced brainâĂŞcomputer interface. *J. Neural Eng.*, 8(4):046035, 2011.

[28] Julie Blumberg, Jörn Rickert, Stephan Waldert, Andreas Schulze-Bonhage, Ad Aertsen, and Carsten Mehring. Adaptive classification for brain computer interfaces. In *Engineering in Medicine and Biology Society, 2007. EMBS 2007. 29th Annual International Conference of the IEEE*, pages 2536–2539. IEEE, 2007.

[29] Dennis J McFarland, William A Sarnacki, and Jonathan R Wolpaw. Should the parameters of a BCI translation algorithm be continually adapted? *J Neuro Methods*, 199(1):103–107, 2011.

[30] Wolfgang HR Miltner, Christoph H Braun, and Michael GH Coles. Event-related brain potentials following incorrect feedback in a time-estimation task: Evidence for a "genericÓ neural system for error detection. *J. Cognitive Neuroscience*, 9(6):788–798, 1997.

[31] William J Gehring and Adrian R Willoughby. The medial frontal cortex and the rapid processing of monetary gains and losses. *Science*, 295(5563):2279–2282, 2002.

[32] Phan Luu, Don M Tucker, Douglas Derryberry, Marjorie Reed, and Catherine Poulsen. Electrophysiological responses to errors and feedback in the process of action regulation. *Psychological Science*, 14(1):47–53, 2003.

[33] Robert M Chapman and Henry R Bragdon. Evoked responses to numerical and non-numerical visual stimuli while problem solving. *Nature*, 203:1155–1157, 1964.

[34] Nancy K Squires, Kenneth C Squires, and Steven A Hillyard. Two varieties of long-latency positive waves evoked by unpredictable auditory stimuli in man. *Electroencephalography and clinical neurophysiology*, 38(4):387–401, 1975.

[35] Stefan Kobza, Patrizia Thoma, Irene Daum, and Christian Bellebaum. The feedback-related negativity is modulated by feedback probability in observational learning. *Behavioural brain research*, 225(2):396–404, 2011.

[36] Michael X Cohen and Charan Ranganath. Reinforcement learning signals predict future decisions. *J. Neuroscience*, 27(2):371–378, 2007.

[37] Lucas C. Parra, Clay D. Spence, Adam D. Gerson, and Paul Sajda. Response error correction - a demonstration of improved human-machine performance using real-time EEG monitoring. *IEEE Trans. Neural Syst. Rehabil. Eng.*, 11(2):173–177, 2003.

[38] S. Jatzev, T.O. Zander, M. DeFlilippis, C. Kothe, S. Welke, and M. Roetting. Examining causes for non-stationarities: The loss of controllability is a factor which induces non-stationarities. In *In Proc. of the 4th Int. BCI Workshop & Training Course*. Graz University of Technology Publishing House, 2008.

[39] T.O. Zander and S. Jatzev. Detecting affective covert user states with passive Brain-Computer Interfaces. In IEEE Computer Society Press, editor, *Proc. of the ACII 2009*, Los Alamitos, CA, 2009.

[40] Pierre W Ferrez and José del R Millan. Error-related EEG potentials generated during simulated brain-computer interaction. *IEEE Trans. Biomed. Eng.*, 55(3):923–929, 2008.

[41] Ricardo Chavarriaga and Jose del R. Millan. Learning from EEG error-related potentials in noninvasive brain-computer interfaces. *IEEE Trans. Neural Syst. Rehabil. Eng.*, 18(4):381–388, 2010.

[42] Xavier Artusi, Imran Khan Niazi, Marie-Françoise Lucas, and Dario Farina. Accuracy of a BCI based on movement-related and error potentials. *Proc. IEEE Eng. Med. Biol. Soc. Conf.*, 2011:3688–91, January 2011.

[43] Alex Kreilinger, Christa Neuper, and Gernot R Müller-Putz. Error potential detection during continuous movement of an artificial arm controlled by brain-computer interface. *Med. Biol. Eng. Comput.*

[44] Ilona Papousek and Günter Schulter. Covariations of EEG asymmetries and emotional states indicate that activity at frontopolar locations is particularly affected by state factors. *Psychophysiology*, 39(3):350–60, May 2002.

[45] H Hinrichs and W Machleidt. Basic emotions reflected in EEG coherences. *Int J Psychophysiol*, 13(3):225–32, Dec 1992.

[46] Irene Winkler, Mark Jäger, Vojkan Mihajlović, and Tsvetomira Tsoneva. Frontal EEG asymmetry based classification of emotional valence using common spatial patterns. *World Academy of Science, Engineering and Technology*, 45:373–378, 2010.

[47] Marni YV Bekkedal, John Rossi, and Jaak Panksepp. Human brain EEG indices of emotions: Delineating responses to affective vocalizations by measuring frontal theta event-related synchronization. *Neuroscience & Biobehavioral Reviews*, 35(9):1959–1970, 2011.

[48] Annekathrin Schacht, Nele Adler, Peiyao Chen, Taomei Guo, and Werner Sommer. Association with positive outcome induces early effects in event-related brain potentials. *Biological psychology*, 89(1):130–136, 2012.

[49] Julie Onton and Scott Makeig. High-frequency broadband modulations of electroencephalographic spectra. *Frontiers in Human Neuroscience*, 3:61, Jan 2009.

[50] Toni Cunillera, Lluís Fuentemilla, Jose Periañez, Josep Marco-Pallarès, Ulrike M Krämer, Estela Càmara, Thomas F Münte, and Antoni Rodríguez-Fornells. Brain oscillatory activity associated with task switching and feedback processing. *Cognitive, Affective, & Behavioral Neuroscience*, 12(1):16–33, 2012.

[51] Sander Nieuwenhuis, Gary Aston-Jones, and Jonathan D Cohen. Decision making, the P3, and the locus coeruleus–norepinephrine system. *Psychological bulletin*, 131(4):510, 2005.

[52] Jouri Perelmouter and Niels Birbaumer. A Binary Spelling Interface with Random Errors. *IEEE Trans. Neural Syst. Rehabil. Eng.*, 8(2):227–232, June 2000.

[53] Vera Ferrari, Margaret M. Bradley, Maurizio Codispoti, and Peter J. Lang. Detecting novelty and significance. *J. Cognitive Neuroscience*, 22(2):404–411, February 2010.

[54] Sven Hoffmann and Michael Falkenstein. Predictive information processing in the brain: Errors and response monitoring. *Int. J. Psychophysiology*, 83(2):208 – 212, 2012.

[55] A. Combaz, N. Chumerin, N.V. Manyakov, A. Robben, J.A.K. Suykens, and M.M. Van Hulle. Towards the detection of error-related potentials and its integration in the context of a p300 speller brain-computer interface. *Neurocomputing*, 80(0):73–82, 2012. Special Issue on Machine Learning for Signal Processing 2010.

[56] Nico M Schmidt, Benjamin Blankertz, and Matthias S Treder. Online detection of error-related potentials boosts the performance of mental typewriters. *BMC Neuroscience*, 13(1):19, February 2012.

[57] Bernardo Dal Seno, Matteo Matteucci, and Luca Mainardi. Online detection of P300 and error potentials in a BCI speller. *Computational Intelligence and Neuroscience*, 2010:307254, January 2010.

[58] Martin Spüler, Michael Bensch, Sonja Kleih, Wolfgang Rosenstiel, Martin Bogdan, and Andrea Kübler. Online use of error-related potentials in healthy users and people with severe motor impairment increases performance of a P300-BCI. *Clinical Neurophysiology*, January 2012.

[59] Arnaud Delorme and Scott Makeig. EEGLAB: an open source toolbox for analysis of single-trial EEG dynamics including independent component analysis. *J. Neuro. Methods*, 134(1):9 – 21, 2004.

[60] Anthony J. Bell and Terrence J. Sejnowski. An information-maximization approach to blind separation and blind deconvolution. *Neural Computation*, 7(6):1129–1159, 1995.

[61] J Müller-Gerking, Gert Pfurtscheller, and H Flyvbjerg. Designing optimal spatial filters for single-trial EEG classification in a movement task. *J. Clin. Neurophysiol.*, 110(5):787–98, May 1999.

[62] Fabien Lotte and Cuntai Guan. Regularizing common spatial patterns to improve BCI designs: Unified theory and new algorithms. *IEEE Trans. Biomed. Eng.*, 58(2):355–362, 2011.

[63] Jerome H. Friedman. Regularized discriminant analysis. *J. Amer. Statistical Association*.

[64] Paul S Hammon and Virginia R de Sa. Preprocessing and meta-classification for brain-computer interfaces. *IEEE Trans. Biomed. Eng.*, 54(3):518–25, Mar 2007.

[65] C. Radhakrishna Rao. The use and interpretation of principal component analysis in applied research. *Sankhya: The Indian Journal of Statistics, Series A*, 26(4):pp. 329–358, 1964.

[66] J.R. Wolpaw, H. Ramoser, D.J. McFarland, and G. Pfurtscheller. EEG-based communication: improved accuracy by response verification. *IEEE Trans. Rehabil. Eng.*., 6(3):326 –333, sep 1998.

[67] GR Müller-Putz, R Scherer, C Brunner, R Leeb, and G Pfurtscheller. Better than random? a closer look on BCI results. *Int. J. Bioelectromagnetism*, 10(1):52–55, 2008.

[68] Brendan Z. Allison and Christa Neuper. Could anyone use a BCI? In Desney S. Tan and Anton Nijholt, editors, *Brain-Computer Interfaces*, Human-Computer Interaction Series, pages 35–54. Springer London, 2010.

[69] Ander Ramos-Murguialday, Markus Scharholz, Vittorio Caggiano, Moritz Wildgruber, Andrea Caria, Eva Maria Hammer, Sebastian Halder, and Niels Birbaumer. Proprioceptive feedback and brain computer interface (BCI) based neuroprostheses. *PLoS ONE*, 7(10):e47048, 10 2012.

[70] Aaron J. Suminski, Dennis C. Tkach, Andrew H. Fagg, and Nicholas G. Hatsopoulos. Incorporating feedback from multiple sensory modalities enhances brain-machine interface control. *The Journal of Neuroscience*, 30(50):16777–16787, 2010.

[71] M. Gonzalez-Franco, Peng Yuan, Dan Zhang, Bo Hong, and Shangkai Gao. Motor imagery based brain-computer interface: A study of the effect of positive and negative feedback. In *Engineering in Medicine and Biology Society,EMBC, 2011 Annual International Conference of the IEEE*, pages 6323 –6326, 30 2011-sept. 3 2011.

[72] Boris Reuderink, Anton Nijholt, and Mannes Poel. Affective pacman: A frustrating game for brain-computer interface experiments. In *Intelligent Technologies for Interactive Entertainment*, pages 221–227. Springer, 2009.

[73] Anne-Marie Brouwer, Maarten A Hogervorst, Jan BF Van Erp, Tobias Heffelaar, Patrick H Zimmerman, and Robert Oostenveld. Estimating workload using EEG spectral power and ERPs in the n-back task. *J. Neural Eng.*, 9(4):045008, 2012.

[74] Michael E Smith, Alan Gevins, Halle Brown, Arati Karnik, and Robert Du. Monitoring task loading with multivariate EEG measures during complex forms of human-computer interaction. *Human Factors: The Journal of the Human Factors and Ergonomics Society*, 43(3):366–380, 2001.

[75] TO Zander and S Jatzev. Context-aware brain–computer interfaces: exploring the information space of user, technical system and environment. *J. Neural Eng.*, 9(1):016003, 2012.

[76] P. Shenoy, M. Krauledat, B. Blankertz, R.P.N. Rao, and K-R. Müller. Towards adaptive classification for BCI. *J. Neural Eng.*, 3:R13–R23, 2006.

[77] Álvaro Barbero and Moritz Grosse-Wentrup. Biased feedback in brain-computer interfaces. *Journal of NeuroEngineering and Rehabilitation*, 7, 2010.

[78] Christa Neuper, Reinhold Scherer, Miriam Reiner, Gert Pfurtscheller, et al. Imagery of motor actions: Differential effects of kinesthetic and visual? motor mode of imagery in single-trial EEG. *Cognitive Brain Research*, 25(3):668–677, 2005.

[79] Zhang-Ye Dong, Dong-Qiang Liu, Jue Wang, Zhao Qing, Zhen-Xiang Zang, Chao-Gan Yan, and Yu-Feng Zang. Low-frequency fluctuation in continuous real-time feedback of finger force: a new paradigm for sustained attention. *Neuroscience bulletin*, 28(4):456–467, 2012.

[80] Zoltan Joseph Koles. The quantitative extraction and topographic mapping of the abnormal components in the clinical EEG. *Electroencephalography and Clinical Neurophysiology*, 79(6):440–447, 1991.

[81] Benjamin Blankertz, Ryota Tomioka, Steven Lemm, Motoaki Kawanabe, and K-R Muller. Optimizing spatial filters for robust EEG single-trial analysis. *Signal Processing Magazine, IEEE*, 25(1):41–56, 2008.

[82] Martin Billinger, Ian Daly, Vera Kaiser, Jing Jin, Brendan Z Allison, Gernot R Müller-Putz, and Clemens Brunner. Is it significant? guidelines for reporting BCI performance. In *Towards Practical Brain-Computer Interfaces*, pages 333–354. Springer, 2013.

[83] Boris Reuderink, Mannes Poel, and Anton Nijholt. The impact of loss of control on movement BCIs. *IEEE Trans. Neural Syst. Rehabil. Eng.*, 19(6):628–637, 2011.

[84] Geoffrey L. Ahern and Gary E. Schwartz. Differential lateralization for positive and negative emotion in the human brain: EEG spectral analysis. *Neuropsychologia*, 23(6):745 – 755, 1985.

[85] Andreas Haag, Silke Goronzy, Peter Schaich, and Jason Williams. Emotion recognition using bio-sensors: First steps towards an automatic system. In Elisabeth André, Laila Dybkj}ae r, Wolfgang Minker, and Paul Heisterkamp, editors, *Affective Dialogue Systems*, Lecture Notes in Computer Science.

[86] Virginia R de Sa. An interactive control strategy is more robust to non-optimal classification boundaries. In *Proceedings of the 14th ACM international conference on Multimodal interaction*, pages 579–586. ACM, 2012.

[87] Benjamin Blankertz, Steven Lemm, Matthias Treder, Stefan Haufe, and Klaus-Robert Müller. Single-trial analysis and classification of ERP components – a tutorial. *NeuroImage*, 56(2):814–825, May 2011.